Geometrical acoustics meets the statistical wave field theory

Roland Badeau

Geometrical acoustics meets the statistical wave field theory

Roland Badeau[a]

[a] *Laboratoire Traitement et Communication de l'Information, Télécom Paris, Institut Polytechnique de Paris, Palaiseau 91120, France*

Abstract

The statistical wave field theory mathematically establishes the statistical laws of the solutions to the wave equation in a bounded domain, which hold at high frequency. It provides the closed-form expressions of the power distribution and the correlations of the wave field jointly over time, frequency and space, in terms of the geometry and the specific admittance of the boundary surface. In our previous article, the mathematical foundations of the theory have been reworked at the fundamental level of the eigenfunctions of the Laplace operator. We thus introduced a random wave model of the complex Robin Laplacian, which accounts for the absortion of energy at the boundary surface. In this article, based on this model, we establish the first and second order statistics of the room impulse response. The previous predictions of the theory are thus retrieved, and their accuracy is improved. In addition, this approach allows us to achieve the unification of geometrical acoustics, which is generally used to predict the first echoes that appear in early reverberation, and of probabilistic models, which are generally used to predict the statistical properties of late reverberation.

Keywords: Statistical physics, wave equation, Helmholtz equation, reverberation

Contents

Email address: roland.badeau@telecom-paris.fr (Roland Badeau)

---

1. Introduction

The statistical wave field theory was originally introduced in Badeau (2024). Its stated goal is to mathematically establish the statistical laws of the solutions to the wave equation in a connected and bounded domain. These laws hold at high frequency, provided that the geometrical shape of the domain satisfies mild assumptions related to chaos. In particular, this theory provides two different kinds of predictions, which are expressed in terms of the geometry and the specific admittance at the boundary surface:

- the isotropic reverberation time in diffuse rooms (Badeau, 2024), and the directional reverberation time in anisotropic wave fields (Badeau, 2026b);
- more generally, the power distribution and the correlations of the wave field jointly over time, frequency and space (Badeau, 2024, 2026b).

The main results obtained so far with this theory were summarized in Badeau (2026c). In particular, the prediction of the reverberation time in diffuse rooms has been verified by experiment, with a remarkable accuracy (Prinn and Badeau, 2026).

The main mathematical tool of the statistical wave field theory is the "B-function", which is a random field that represents the distribution of image sources over space at fixed wave number k. This random field is real-valued when there is no energy absorption at the domain's boundary, and it is complex-valued when there is energy absorption. From the statistics of this B-function, the statistics of the Green's function of the Helmholtz equation are derived, from which the statistics of the room response to a punctual source are finally deduced.

In this paper, the mathematical foundations of the theory are reworked at a more fundamental level than that of the B-function. Indeed, our new assumptions focus on the statistical properties of the eigenspectrum and eigenfunctions of the complex Robin Laplacian, from which the B-function is defined. Based on the *random wave model* (RWM) of the complex Robin Laplacian recently introduced in Badeau (2026d), this new approach will turn out to be extremely powerful: not only will we retrieve all the previous predictions of the theory, and improve the accuracy of the predicted power distribution in the case of energy absorption, but we will also end up with an unexpected and remarkable result. Indeed, this new approach will allow us to achieve the unification of geometrical acoustics (Kuttruff, 2014, Chap. 4), which is generally used to predict the first echoes that appear in early reverberation, and of probabilistic models (Kuttruff, 2014, Chap. 5), which are generally used to predict the statistical properties of late reverberation. More precisely, the direct path and the first echos will be retrieved in the first order statistics of the B-function, through the spatial distribution of the first image sources, and in the first order statistics of the *room impulse response* (RIR), through a sum of spherical waves emitted by these image sources. In addition, the power distribution of late reverberation will be retrieved, as in our previous works, in the second order statistics of the B-function and of the RIR. Finally, we will show that the former third assumption of the statistical wave field theory, which states that the mean and pseudo-covariances of the B-function are stationary (Badeau, 2024), becomes a mathematical result, proved from the more fundamendal assumptions on the eigenspectrum and eigenfunctions of the Robin Laplacian.

This paper is organized as follows. In the next section, we introduce some acronyms and mathematical notations that will be used in the rest of the paper. Then in Sec. 2, we summarize a few fundamental notions regarding wave propagation that are needed to develop the statistical wave field theory. In Sec. 3, we present an overview of the proposed contribution, in relation to several related works from the existing literature. In Sec. 4, we investigate the first and second order statistics of the wave field, which result from the RWM introduced in Badeau (2026d, Sec. IV). Finally, in Sec. 5 we summarize the main contributions of this paper, compare our results with existing works, and present a few perspectives for future work. This paper also contains two appendices. In Appendix A, we show that the B-function converges almost surely to a distribution, and we prove the former third assumption of the statistical wave field theory, based on the RWM introduced in Badeau (2026d, Sec. IV). Then in Appendix B, we calculate the first and second order statistics of the RIR.

Acronyms and mathematical notations

Acronyms:

ACF Auto-covariance function

GOE Gaussian orthogonal ensemble

PCF Pseudo-covariance function

PDE Partial differential equation

PSD Power spectral density

RIR Room impulse response

RWM Random wave model

Mathematical notations:

In this paper, we use the same mathematical notations as in Badeau (2026d, Sec. I). In addition, the Greek letter ψ is used to denote *any function of any variables* (we do not use the notation f that is usual in mathematics, because here f denotes the frequency). Therefore, the same letter ψ may denote different functions of different variables in different places of the paper, and it is not supposed to have any special physical meaning.

2. Fundamentals of waves revisited

This section summarizes a few fundamental notions regarding wave propagation that are needed in the rest of the paper. Most of these notions are well-known and are described for instance in Morse and Ingard (1968). These and other notions were already presented in more details in Badeau (2024, Sec. III).

2.1. Main definitions

In a connected open domain $V \subseteq \mathbb{R}^3$, the homogeneous wave equation states that

$$\Delta p(\boldsymbol{x}, t) - \tfrac{1}{c^2} \tfrac{\partial^2 p(\boldsymbol{x},t)}{\partial t^2} = 0, \tag{1}$$

where $p(\boldsymbol{x}, t)$ is the wave amplitude at position $\boldsymbol{x} \in V$ and time $t \in \mathbb{R}$, Δ is the Laplacian, and c is the propagation speed. Applying the Fourier transform w.r.t. time to Eq. (1) yields the Helmholtz equation:

$$\Delta\varphi(\boldsymbol{x}) + 4\pi^2 k^2 \varphi(\boldsymbol{x}) = 0, \tag{2}$$

where the scalar $k = \frac{f}{c}$ is the *wave number* and f denotes the frequency. Any solution φ to Eq. (2) is an eigenfunction of the Laplace operator $-\Delta$, of eigenvalue $4\pi^2 k^2$.

Given a punctual source position $\boldsymbol{x}^s \in V$ and a receiver position $\boldsymbol{x}^r \in V$, the RIR $h(\boldsymbol{x}^r, \boldsymbol{x}^s, t)$ is defined as the unique causal solution to the following inhomogeneous wave equation: $\forall t \in \mathbb{R}$,

$$\Delta_{\boldsymbol{x}^r} h(\boldsymbol{x}^r, \boldsymbol{x}^s, t) - \tfrac{1}{c^2}\tfrac{\partial^2 h(\boldsymbol{x}^r, \boldsymbol{x}^s, t)}{\partial t^2} = -\delta(\boldsymbol{x}^r - \boldsymbol{x}^s)\delta(t), \tag{3}$$

where δ denotes the Dirac delta function. In the free field (i.e., when $V = \mathbb{R}^3$), h is expressed as

$$h(\boldsymbol{x}^r, \boldsymbol{x}^s, t) = \frac{\delta\left(t - \frac{\|\boldsymbol{x}^r - \boldsymbol{x}^s\|_2}{c}\right)}{4\pi\|\boldsymbol{x}^r - \boldsymbol{x}^s\|_2}. \tag{4}$$

2.2. Green's function

Given a punctual source position $\boldsymbol{x}^s \in V$ and a receiver position $\boldsymbol{x}^r \in V$, a Green's function G of the Helmholtz equation is a particular solution to the following inhomogeneous Helmholtz equation:

$$\Delta_{\boldsymbol{x}^r} G(\boldsymbol{x}^r, \boldsymbol{x}^s, k) + 4\pi^2 k^2 G(\boldsymbol{x}^r, \boldsymbol{x}^s, k) = -\delta(\boldsymbol{x}^r - \boldsymbol{x}^s). \tag{5}$$

The inverse 1D Fourier transform of G w.r.t. frequency $f = ck$,

$$g(\boldsymbol{x}^r, \boldsymbol{x}^s, t) = \int_{f\in\mathbb{R}} G(\boldsymbol{x}^r, \boldsymbol{x}^s, \tfrac{f}{c})\, e^{2\imath\pi f t} df, \tag{6}$$

is a solution to Eq. (3). However, depending on the choice of a particular solution G to Eq. (5), the function $g(\boldsymbol{x}^r, \boldsymbol{x}^s, t)$ may not be causal, so in general $g(\boldsymbol{x}^r, \boldsymbol{x}^s, t)$ differs from the causal RIR $h(\boldsymbol{x}^r, \boldsymbol{x}^s, t)$ by a function that is a solution to the homogeneous wave equation [Eq. (1)].

In the free field ($V = \mathbb{R}^3$), any Green's function G solution to Eq. (5) can be written as the translation over space of some Green's function G_0 for a source located at $\boldsymbol{x}^s = \mathbf{0}$:

$$G(\boldsymbol{x}^r, \boldsymbol{x}^s, k) = G_0(\boldsymbol{x}^r - \boldsymbol{x}^s, k).$$

In this paper, we will consider the real Green's function

$$G_0(\boldsymbol{z}, k) = \frac{\cos(2\pi k\|\boldsymbol{z}\|_2)}{4\pi\|\boldsymbol{z}\|_2}, \tag{7}$$

which is such that function g in Eq. (6) is an even function of time.

2.3. B-function

In the case of a connected domain $V \subset \mathbb{R}^3$ with boundaries, any Green's function $G(\boldsymbol{x}^r, \boldsymbol{x}^s, k)$ can generally be analytically continued in a mathematical vicinity $\mathcal{D}$ of V that depends on the domain's geometry and the boundary condition. In some cases, this extension holds in the full space $\mathcal{D} = \mathbb{R}^3$. The B-function on $\mathcal{D} \subseteq \mathbb{R}^3$ is then defined as:

$$B(\boldsymbol{y}^r, \boldsymbol{x}^s, k) = -\left(\Delta_{\boldsymbol{y}^r} G(\boldsymbol{y}^r, \boldsymbol{x}^s, k) + 4\pi^2 k^2 G(\boldsymbol{y}^r, \boldsymbol{x}^s, k)\right). \tag{8}$$

By definition of the Green's function G in Eq. (5), the restriction of the B-function to V is $\delta(\boldsymbol{y}^r - \boldsymbol{x}^s)$. Reciprocally, when $\mathcal{D} = \mathbb{R}^3$, a particular Green's function G is obtained as:

$$G(\boldsymbol{x}^r, \boldsymbol{x}^s, k) = \int_{\boldsymbol{y}^r \in \mathbb{R}^3} G_0(\boldsymbol{x}^r - \boldsymbol{y}^r, k)\, B(\boldsymbol{y}^r, \boldsymbol{x}^s, k) d\boldsymbol{y}, \tag{9}$$

where G_0 is a free-field Green's function. Equation (9) permits us to interpret the B-function as a spatial distribution of image sources in the free field, which collectively generate inside V the same response as that of the single original source within the bounded domain V.

2.4. Boundary condition

Let us now consider a connected domain $V \subset \mathbb{R}^3$, whose boundary ∂V is a Lipschitz continuous bidimensional (2D) manifold (i.e., ∂V is locally the graph of a Lipschitz function). The boundary ∂V is characterized by the *specific admittance* $\widehat{\beta}(\boldsymbol{s}, k) \in \mathbb{C}$, which is an essentially bounded function of the position $\boldsymbol{s} \in \partial V$. Then, Robin's boundary condition of Eq. (2) states that

$$\forall \boldsymbol{s} \in \partial V,\ \tfrac{\partial \varphi(\boldsymbol{s},k)}{\partial \boldsymbol{n}(\boldsymbol{s})} + 2\imath\pi k \widehat{\beta}(\boldsymbol{s}, k)\varphi(\boldsymbol{s}, k) = 0, \tag{10}$$

where $\frac{\partial}{\partial \boldsymbol{n}(\boldsymbol{s})}$ denotes partial differentiation in the direction of the outward normal $\boldsymbol{n}(\boldsymbol{s})$ to the boundary surface at $\boldsymbol{s}$. This boundary condition explicitly depends on k, so Eq. (2) has to be rewritten

$$\Delta\varphi(\boldsymbol{x}, k) + 4\pi^2\kappa(k)^2\varphi(\boldsymbol{x}, k) = 0, \tag{11}$$

where the wave number is now denoted $\kappa(k) \in \mathbb{C}$. In the case of *non-rigid* surfaces, which absorb a part of the energy of the incident wave, $\widehat{\beta}(\boldsymbol{s}, k) \in \mathbb{C}$ and $\mathrm{Re}(\widehat{\beta}(\boldsymbol{s}, k)) > 0$. Then the Robin Laplace operator $-\Delta$ is complex and not self-adjoint, and when the domain V is bounded, the set of (generalized) eigenvalues and eigenfunctions is discrete and complex, and it was proved in Badeau (2025a) that the (generalized) eigenfunctions can be chosen to form a pseudo-orthonormal *Abel basis with brackets* of the Hilbert space $L^2(V)$, a notion that is defined in Badeau (2025a, Sec. III A). However, when there is no energy absorption, $\widehat{\beta}(\boldsymbol{s}, k)$ is purely imaginary, the Robin Laplace operator is real and self-adjoint, the set of eigenvalues and eigenfunctions is discrete and real, and the eigenfunctions can be chosen to form an orthonormal basis of $L^2(V)$. In particular, when $\widehat{\beta}(\boldsymbol{s}, k) = 0$, Eq. (10) reduces to Neumann's boundary condition.

3. Overview of the contribution in relation to existing works

In this section, we review and comment the existing probabilistic models of the eigenspectrum (Sec. 3.1) and eigenfunctions (Sec. 3.2) of the Robin Laplacian that are related to the statistical wave field theory, as well as the consistency between these various models (Sec. 3.3). We also briefly present the cross-Wigner time-frequency distribution (Sec. 3.4), which will be used to characterize the non-stationary second order statistics of the RIR in Sec. 4.3.3.

3.1. *Eigenspectrum of the real Robin Laplacian*

Let us first focus on the properties of the discrete eigenspectrum $\{\kappa_n(k)\}_{n\in\mathbb{N}}$, which is such that the eigenvalues of the Laplace operator $-\Delta$ are $\lambda_n(k) = 4\pi^2\kappa_n(k)^2$.

3.1.1. *Asymptotic expansion of the modal density*

At high frequency, the discrete eigenspectrum of the real Robin Laplacian is well described by a smooth density function $\rho(\kappa, k)$. In several dimensions of space, it is well known that $\rho(\kappa, k)$ increases with κ, in a way that has been investigated mathematically for the first time by Weyl (1911). Weyl's formula is an asymptotic expansion that holds when $\kappa \to +\infty$. In three space dimensions, with our notations, it can be expressed in the following form:

$$\rho(\kappa, k) = 4\pi|V|\kappa^2. \tag{12}$$

The dominant term is proportional to the volume of the domain V, and is thus called the *volume* term. The remaining terms (omitted in Eq. (12)) are of order $O(\kappa)$. Later, the physicists Balian and Bloch (1970) derived the two following terms of this asymptotic expansion, which are called *surface* term and *curvature* term, respectively. With our notations, up to the first order surface term, their asymptotic expansion can be written as:

$$\rho(\kappa, k) = 4\pi|V|\kappa^2 + \kappa\left(\frac{\pi S(\partial V)}{2} + \imath\int_{\boldsymbol{s}\in\partial V}\ln\left(\frac{\kappa - k\widehat{\beta}(\boldsymbol{s},k)}{\kappa + k\widehat{\beta}(\boldsymbol{s},k)}\right)dS(\boldsymbol{s})\right), \tag{13}$$

where the right member is real-valued, because $\widehat{\beta} \in \imath\mathbb{R}$. Their mathematical approach was based on a *multiple reflection expansion* of the Green's function. It is important to note that the volume term is related to the direct path in this multiple reflection expansion, the surface term (which corresponds to the integral over the boundary surface ∂V in Eq. (13)) is related to the first order reflections, and the curvature term, of order $O(1)$ (which is omitted in Eq. (13)), additionally includes second order reflections.

Later, the periodic orbit theory showed that each periodic orbit (also called "closed path" by Balian and Bloch (1972)), of length L in the classical billiard, produces a fluctuation of period c/L in the modal density, which is expressed by the Gutzwiller trace formula (Gutzwiller, 1971). In this regard, Eq. (13) provides a *mean level density*, which can be interpreted as the result of smoothing the exact oscillating density, by applying a smoothing filter of bandwidth much larger than $1/L_{\min}$, where $L_{\min}$ is the fundamental period of the shortest classical periodic orbit.

3.1.2. *Wave number distortion*

In Badeau (2024), we showed that in the case of ergodic billiards, Eq. (13) induces a *wave number distortion* between the Neumann and Robin boundary conditions. More precisely, if the Neumann and Robin wave numbers are denoted K and $\mathcal{K}(K, k)$, respectively, then function $\mathcal{K}(K, k)$ is defined as the unique solution to the equation

$$\forall K > 0,\ \rho(\mathcal{K}(K, k), k)\,\frac{\partial\mathcal{K}(K,k)}{\partial K} = \rho(K, 0). \tag{14}$$

From Eqs. (13) and (14), we were able to derive its first order asymptotic expansion (Badeau, 2024, Eq. (102)):

$$\begin{aligned}\mathcal{K}(K,k) = K + \tfrac{\imath\lambda}{8\pi}\int_{\boldsymbol{s}\in\partial V}\Bigg(&\ln\left(\tfrac{\mathcal{K}(K,k)+k\widehat{\beta}(\boldsymbol{s},k)}{\mathcal{K}(K,k)-k\widehat{\beta}(\boldsymbol{s},k)}\right)\\ -\left(\tfrac{k\widehat{\beta}(\boldsymbol{s},k)}{\mathcal{K}(K,k)}\right)^2\ln\left(\tfrac{k\widehat{\beta}(\boldsymbol{s},k)+\mathcal{K}(K,k)}{k\widehat{\beta}(\boldsymbol{s},k)-\mathcal{K}(K,k)}\right) &+ \tfrac{2k\widehat{\beta}(\boldsymbol{s},k)}{\mathcal{K}(K,k)}\Bigg)dS(\boldsymbol{s}),\end{aligned} \tag{15}$$

where $\lambda \triangleq \frac{1}{|V|}$ is the inverse of the room's volume. A remarkable property of Eq. (15) is that, by analytic continuation, it still holds in the general case of the *complex* Robin Laplacian, even though $\rho(\kappa,k)$ can no longer be interpreted as a modal density in this case, since the parameter κ is complex. Moreover, we showed that Eq. (15) leads to a closed-form expression of the reverberation time in mixing rooms (Badeau, 2024, Eq. (124)) that has been verified by experiment (Prinn and Badeau, 2026). By applying the same method up to the second order curvature term investigated by Balian and Bloch (1970), we were also able to get the second order asymptotic expansion of function $\mathcal{K}(K,k)$, and the resulting closed-form expression of the reverberation time (Badeau, 2025b, Eq. (52)).

3.1.3. Probability distribution of the eigenspectrum

In Sec. 3.1.1, we focused on the mean level modal density, which results from applying spectral smoothing to the discrete eigenspectrum of the real Robin Laplacian. Beyond this modal density, it is also interesting to investigate the fine distribution of the individual eigenfrequencies in this discrete spectrum. In the literature on chaotic billiards, it is well known that these eigenfrequencies follow the same probability distribution as that of the eigenvalues of random matrices from the *Gaussian Orthogonal Ensemble* (GOE) (Tanner and Søndergaard, 2007, Sec. 3). The discrete eigenspectrum $\{\kappa_n(k)\}_{n\in\mathbb{N}}$ can then be modeled as a random point process, which can be represented as a random measure on $\mathbb{R}_+$:

$$\mu(\kappa,k) = \sum_{n\in\mathbb{N}}\delta(\kappa-\kappa_n(k)). \tag{16}$$

This measure μ is such that for any continuous function ψ defined on $\mathbb{R}_+$,

$$\sum_{n\in\mathbb{N}}\psi(\kappa_n(k)) = \int_{\kappa\in\mathbb{R}_+}\psi(\kappa)\,d\mu(\kappa,k)$$

is a random variable, whose mathematical expectation is expressed as

$$\mathbb{E}\left[\int_{\kappa\in\mathbb{R}_+}\psi(\kappa)d\mu(\kappa,k)\right] = \int_{\kappa\in\mathbb{R}_+}\psi(\kappa)\rho(\kappa,k)d\kappa, \tag{17}$$

where $\rho(\kappa,k)$ is the modal density introduced in Sec. 3.1.1. In addition, for two continuous functions ψ_1 and ψ_2 defined on $\mathbb{R}_+$, we have

$$\begin{aligned}&\mathbb{E}\left[\int_{\kappa_1\in\mathbb{R}_+}\psi_1(\kappa_1)d\mu(\kappa_1,k)\int_{\kappa_2\in\mathbb{R}_+}\psi_2(\kappa_2)d\mu(\kappa_2,k)\right]\\ &=\iint_{\kappa_1,\kappa_2\in\mathbb{R}_+}\psi_1(\kappa_1)\,\psi_2(\kappa_2)\\ &R_2\left((\kappa_1-\kappa_2)\rho\left(\tfrac{\kappa_1+\kappa_2}{2},k\right)\right)\rho(\kappa_1,k)\,\rho(\kappa_2,k)\,d\kappa_1 d\kappa_2,\end{aligned} \tag{18}$$

where $R_2(s)$ denotes the rescaled *two-point correlation function* (Tanner and Søndergaard, 2007, p. R476). By substituting Eqs. (17) and (18), and by applying the change of variables $\kappa_1 = \kappa + \frac{s}{2\rho(\kappa,k)}$ and $\kappa_2 = \kappa - \frac{s}{2\rho(\kappa,k)}$, we then get

$$\begin{aligned}&\operatorname{cov}\left[\int_{\kappa_1\in\mathbb{R}_+} \psi_1(\kappa_1) d\mu(\kappa_1, k), \int_{\kappa_2\in\mathbb{R}_+} \psi_2(\kappa_2) d\mu(\kappa_2, k)\right] \\ &= \int_{\kappa\in\mathbb{R}_+} \left(\int_{s\in\mathbb{R}} \psi_1\left(\kappa + \frac{s}{2\rho(\kappa,k)}\right) \psi_2\left(\kappa - \frac{s}{2\rho(\kappa,k)}\right) \right. \\ &\left. (R_2(s) - 1)\, ds \right) \rho(\kappa, k) d\kappa,\end{aligned} \tag{19}$$

where we have substituted $d\kappa_1 d\kappa_2 = \frac{d\kappa ds}{\rho(\kappa,k)}$, and $\frac{\rho\left(\kappa+\frac{s}{2\rho(\kappa,k)},k\right)\rho\left(\kappa-\frac{s}{2\rho(\kappa,k)},k\right)}{\rho(\kappa,k)} = \rho(\kappa, k)$, which hold asymptotically when $\kappa \to +\infty$.

The *level cluster function* Y is then defined as (Tanner and Søndergaard, 2007, p. R477)

$$Y(s) = 1 - R_2(s), \tag{20}$$

which is a real and even function. Classical results from the random matrix theory (Mehta, 1991) show that the *form factor* $b \triangleq \widehat{Y}$, defined as the real and even Fourier transform of Y, is expressed as (Weaver and Lobkis, 2000)

$$b(\tau) = \begin{cases} 1 - 2\tau + \tau \ln(2\tau + 1) & \text{for } 0 \leq \tau \leq 1; \\ -1 + \tau \ln\left(\frac{2\tau+1}{2\tau-1}\right) & \text{for } 1 < \tau. \end{cases} \tag{21}$$

Function $b(\tau)$ is plotted in Fig. 1. It is positive and decreasing on $\mathbb{R}_+$, between $b(0) = 1$ and $\lim_{\tau\to+\infty} b(\tau) = 0$. More precisely, $b(\tau) = O(\frac{1}{\tau^2})$ when $\tau \to +\infty$, therefore $b \in L^1(\mathbb{R})$, which implies that function Y is continuous and bounded. In the same way, the first and second order derivatives of b belong to $L^1(\mathbb{R})$. In addition, function b is continuously differentiable at $\tau = 1$, and smooth on $\mathbb{R}_+\backslash\{1\}$. This implies that $Y(s) = O(\frac{1}{s^2})$ when $|s| \to +\infty$.

3.2. Eigenfunctions of the Robin Laplacian

After having investigated the properties of the eigenspectrum of the real Robin Laplacian in Sec. 3.1, we now focus on its eigenfunctions $\{\varphi_n(\boldsymbol{x}, k)\}_{n\in\mathbb{N}}$. More precisely, as in Badeau (2026d, Sec. III), we will investigate the statistical properties of certain functionals of the eigenfunctions related to mixing billiards, which are averaged over a small bandwidth. For instance, we will be interested in averages of the form

$$\mathcal{F}^{(1)}(\boldsymbol{x}, \kappa, k) = \frac{\sum\limits_{\{n\in\mathbb{N}:\, \kappa-\frac{\epsilon}{2}\leq\kappa_n(k)<\kappa+\frac{\epsilon}{2}\}} \varphi_n(\boldsymbol{x},k)}{\int_{\kappa-\frac{\epsilon}{2}}^{\kappa+\frac{\epsilon}{2}} \rho(\kappa',k)d\kappa'}, \tag{22}$$

and

$$\mathcal{F}^{(2)}(\boldsymbol{x}_1, \boldsymbol{x}_2, \kappa, k) = \frac{\sum\limits_{\{n\in\mathbb{N}:\, \kappa-\frac{\epsilon}{2}\leq\kappa_n(k)<\kappa+\frac{\epsilon}{2}\}} \varphi_n(\boldsymbol{x}_1,k)\, \varphi_n(\boldsymbol{x}_2,k)}{\int_{\kappa-\frac{\epsilon}{2}}^{\kappa+\frac{\epsilon}{2}} \rho(\kappa',k)d\kappa'}, \tag{23}$$

for a given bandwidth $\epsilon > 0$. Note that this kind of spectral averaging is related to the spectral smoothing of the modal density that we mentioned at the end of Sec. 3.1.1, and

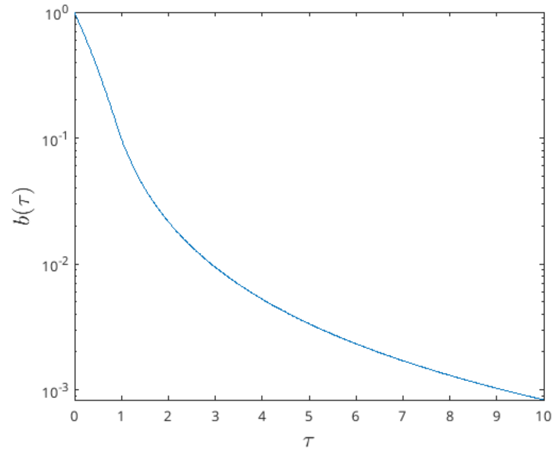

Figure 1: Plot of the form factor $b(\tau)$ expressed in Eq. (21) (blue curve)

it is also related to the eigenstate stacking theorem (Lu *et al.*, 2025), which characterizes the statistical properties in phase space of sums of eigenfunctions, under the same minimal bandwidth condition ($\epsilon > 1/L_{\min}$, where $L_{\min}$ is the fundamental period of the shortest classical periodic orbit). Indeed, due to Eq. (13), when ϵ is fixed and $\kappa \to +\infty$, the number of terms involved in the averages in Eqs. (22) and (23) tends to infinity. These averages then become statistically insensitive to certain anomalies that may appear in some rare eigenfunctions, such as quantum scars (Lu *et al.*, 2025). The statistical properties of $\mathcal{F}^{(1)}(\boldsymbol{x}, \kappa, k)$ and $\mathcal{F}^{(2)}(\boldsymbol{x}_1, \boldsymbol{x}_2, \kappa, k)$ then become regular, and can be described by simple probabilistic models.

In the literature, various RWMs have thus been proposed, which generally represent the eigenfunctions $\varphi_n(\boldsymbol{x}, k)$ as centered and pairwise independent random fields (Urbina and Richter, 2006). In particular, the independence of the eigenfunctions is consistent with the quantum weak mixing theorem in phase space for classically weak mixing billiards (Zelditch, 2006) (see Badeau (2026a, Sec. I) for more details on this topic). From now on, we will thus write equations such as $\mathbb{E}[\varphi_n(\boldsymbol{x}, k)] = 0$, and $\forall n_1 \neq n_2$, $\mathrm{cov}[\varphi_{n_1}(\boldsymbol{x}_1, k_1)\, \varphi_{n_2}(\boldsymbol{x}_2, k_2)] = 0$, which might misleadingly suggest that we are focusing on individual eigenfunctions. The reader should keep in mind that these equations implicitly involve spectral averages, like in Eqs. (22) and (23). Nevertheless, this simplified probabilistic notation will prove to be very useful, and it will allow us to get accurate predictions of the wave field statistics.

3.2.1. Gaussian distribution

It was originally conjectured by Berry (1977) that the eigenfunctions of classically chaotic systems can be represented as a random superposition of plane waves with fixed wave number. Then, due to the central limit theorem, these eigenfunctions have the same statistics as a Gaussian random field (Urbina and Richter, 2007). This conjecture was originally formulated for the real eigenfunctions of the real Robin Laplacian, but in fact the same argument applies to the complex eigenfunctions of the complex Robin Laplacian. In Badeau (2026d, Sec. IV), we showed that the Gaussian distribution of these complex eigenfunctions is characterized by the following covariances, for two possibly different values of k_1 and k_2,

$$\operatorname{cov}\left[\varphi_n(\boldsymbol{x}_1, k_1), \varphi_n(\boldsymbol{x}_2, k_2)\right] = \lambda\gamma(\boldsymbol{x}_1, \boldsymbol{x}_2, K_n, k_1, k_2), \tag{24}$$

where K_n denotes the wave number related to Neumann's boundary condition, and the following pseudo-covariances, for $k_1 = k_2 = k$:

$$\operatorname{cov}\left[\varphi_n(\boldsymbol{x}_1, k), \overline{\varphi_n(\boldsymbol{x}_2, k)}\right] = \lambda C(\boldsymbol{x}_1, \boldsymbol{x}_2, \mathcal{K}(K_n, k), k), \tag{25}$$

where $\mathcal{K}(K_n, k)$ is the wave number distortion introduced in Sec. 3.1.2. In the particular case of the real Robin Laplacian, for $k_1 = k_2 = k$, we get $\gamma(\boldsymbol{x}_1, \boldsymbol{x}_2, K, k, k) = C(\boldsymbol{x}_1, \boldsymbol{x}_2, \mathcal{K}(K, k), k) \in \mathbb{R}$.

In other respects, a consequence of the Gaussian assumption is that the fourth order moments, involving either the eigenfunctions or their conjugates, can easily be deduced from Eqs. (24) and (25), thanks to the following lemma (Janssen and Stoica, 1988):

Lemma 1. *For any jointly Gaussian complex random variables Z_1, Z_2, Z_3, Z_4,*

$$\begin{aligned}\mathbb{E}\left[Z_1\, Z_2\, Z_3\, Z_4\right] = \;& \mathbb{E}\left[Z_1\, Z_2\right]\, \mathbb{E}\left[Z_3\, Z_4\right] + \mathbb{E}\left[Z_1\, Z_3\right]\, \mathbb{E}\left[Z_2\, Z_4\right] \\ & + \mathbb{E}\left[Z_1\, Z_4\right] \mathbb{E}\left[Z_2\, Z_3\right] - 2\mathbb{E}\left[Z_1\right] \mathbb{E}\left[Z_2\right] \mathbb{E}\left[Z_3\right] \mathbb{E}\left[Z_4\right].\end{aligned}$$

3.2.2. Universal (pseudo-)correlation functions

Real Robin Laplacian. The correlation function predicted by Berry (1977) is given by the well-known spherical Bessel function:

$$C(\boldsymbol{x}_1, \boldsymbol{x}_2, \kappa, k) = \operatorname{sinc}\left(2\pi\kappa \|\boldsymbol{x}_1 - \boldsymbol{x}_2\|_2\right), \tag{26}$$

where notation C was introduced in Eq. (25). Note that this expression is actually independent of k. This function is often referred to as the *universal correlation function* (Urbina and Richter, 2007), because it applies to any ergodic billiard, independently of its particular geometrical shape.

Equation (26) models the eigenfunctions as isotropically distributed, stationary random fields, which is consistent with the quantum ergodicity theorem in phase space for classically ergodic billiards (Zelditch and Zworski, 1996), and with the eigenstate stacking theorem (Lu *et al.*, 2025) (see Badeau (2026a, Sec. I) for more details on this topic). However, even though Eq. (26) does hold when the two points $\boldsymbol{x}_1$ and $\boldsymbol{x}_2$ are close enough, it was proved inaccurate when the distance between $\boldsymbol{x}_1$ and $\boldsymbol{x}_2$ is not much smaller than their distances to the boundary (see Sec. 3.2.4).

Complex Robin Laplacian. In Badeau (2026d, Sec. IV C), we showed that in the general case of the complex Robin Laplacian, the analytic continuation of function $C(\boldsymbol{x}_1, \boldsymbol{x}_2, \kappa, k)$ defined in Eq. (26) to complex values of the wave number κ still satisfies Eq. (25), which describes the pseudo-covariances of the eigenfunctions. Function $C(\boldsymbol{x}_1, \boldsymbol{x}_2, \kappa, k)$ is then referred to as the *universal pseudo-correlation function*. In particular, for $\boldsymbol{x}_1 = \boldsymbol{x}_2 = \boldsymbol{x}$, Eqs. (25)

and (26) yield $\mathbb{E}[\varphi_n(\boldsymbol{x},k)^2] = \lambda$, which shows that the random wave model respects the (pseudo)-normality of the eigenfunctions:

$$\mathbb{E}\left[\int_{\boldsymbol{x}\in V} \varphi_n(\boldsymbol{x},k)^2 d\boldsymbol{x}\right] = 1. \tag{27}$$

In addition, still in the complex case, the *universal correlation function* γ that was introduced in Eq. (24) is expressed as (Badeau, 2026d, Eq. (24)):

$$\begin{array}{rl} & \gamma(\boldsymbol{x}_1,\boldsymbol{x}_2,K,k_1,k_2) \\ = & \frac{1}{4\pi}\int_{\boldsymbol{u}\in\mathcal{S}(0,1)} e^{\imath 2\pi \boldsymbol{u}^\top\left(\mathcal{K}(K,k_1)\boldsymbol{x}_1 - \overline{\mathcal{K}(K,k_2)}\boldsymbol{x}_2\right)} \\ & \times e^{\imath\left(\theta(\boldsymbol{u},K,k_1)-\overline{\theta(\boldsymbol{u},K,k_2)}\right)}\, dS(\boldsymbol{u}). \end{array} \tag{28}$$

In Eq. (28), function $\boldsymbol{u}\mapsto\theta(\boldsymbol{u},K,k)$ is the *phase distortion*, which is defined as the unique odd solution to the following equation (Badeau, 2026d, Eq. (16)): $\forall K>0$, $\forall \boldsymbol{u}\in\mathcal{S}(0,1)$,

$$\begin{array}{rl} & \lambda\int_{\boldsymbol{s}\in\partial V}\theta(\boldsymbol{u},K,k)-\theta(\boldsymbol{R}(\boldsymbol{s})\boldsymbol{u},K,k)dS(\boldsymbol{s}) \\ = & -2\pi(\mathcal{K}(K,k)-K)\boldsymbol{u}^\top \\ & \times\left(2\lambda\int_{\boldsymbol{s}\in\partial V}\left(\boldsymbol{n}(\boldsymbol{s})\boldsymbol{n}(\boldsymbol{s})^\top\boldsymbol{s}\right)dS(\boldsymbol{s})\right) \\ & +\imath\lambda\int_{\boldsymbol{s}\in\partial V}\ln\left(\frac{\mathcal{K}(K,k)\,\boldsymbol{u}^\top\boldsymbol{n}(\boldsymbol{s})+k\widehat{\beta}(\boldsymbol{s},k)}{\mathcal{K}(K,k)\,\boldsymbol{u}^\top\boldsymbol{n}(\boldsymbol{s})-k\widehat{\beta}(\boldsymbol{s},k)}\right)dS(\boldsymbol{s}), \end{array} \tag{29}$$

where $\boldsymbol{n}(\boldsymbol{s})$ is the outward normal to the boundary surface at $\boldsymbol{s}$, and $\boldsymbol{R}(\boldsymbol{s})$ denotes the reflection matrix w.r.t. the 2D subspace parallel to the plane tangent to ∂V at $\boldsymbol{s}$: $\boldsymbol{R}(\boldsymbol{s}) = \boldsymbol{I} - 2\,\boldsymbol{n}(\boldsymbol{s})\,\boldsymbol{n}(\boldsymbol{s})^\top$, where $\boldsymbol{I}$ is the identity matrix. In practice, Eq. (29) can be solved by decomposing function θ as a series of spherical harmonics, as shown in Badeau (2026d, Sec. IV B).

3.2.3. Enhanced backscattering

Let us focus again on the real Robin Laplacian in an ergodic billiard. We have seen in Sec. 3.2.2 that the universal correlation function represents every eigenfunction of the real Robin Laplacian in an ergodic billiard as a stationary random field. This property suggests that the wave field that results from the combination of all eigenfunctions is itself stationary at high frequency. And indeed, the asymptotic statistics of the RIR prove to be stationary over space, but in practice this property only holds *far enough from the original source position*. On the contrary, at this specific position, the intensity of the wave field is enhanced by a factor ranging from 2 to 3 over time, a phenomenon that is known as *enhanced backscattering* in acoustics (Weaver and Lobkis, 2000).

Mathematically, if we jointly consider the probability distribution of the eigenspectrum introduced in Sec. 3.1.3, the Gaussian model introduced in Sec. 3.2.1, and the universal correlation function introduced in Sec. 3.2.2, then, by applying Lemma 1, it can be proved that (Weaver and Lobkis, 2000)

$$\begin{array}{l} \mathbb{E}\left[\varphi_n(\boldsymbol{x}^r,k)^2\varphi_n(\boldsymbol{x}^s,k)^2\right] = \\ \lambda^2\left(1+(2-b(\frac{t}{t_H(\kappa_n(k),k)}))C(\boldsymbol{x}^r,\boldsymbol{x}^s,\mathcal{K}(K_n,k),k)^2\right), \end{array} \tag{30}$$

where $\boldsymbol{x}^s$ and $\boldsymbol{x}^r$ denote the source and receiver positions, respectively, and the form factor b was defined in Eq. (21) and represented in Fig 1. In Eq. (30),

$$t_H(\kappa, k) = \tfrac{\rho(\kappa,k)}{c} \tag{31}$$

is called the *Heisenberg time.* Note that when $t \to +\infty$ and $t_H(\kappa, k)$ is fixed, then $b\left(\frac{t}{t_H(\kappa,k)}\right) \to 0$. However, $t_H(\kappa, k)$ is proportional to the modal density, and thus grows quadratically with the wave number. So, because we consider both large times t and large wave numbers κ in this paper, two different asymptotics are actually possible:

- if $t \gg \frac{|V|\kappa^2}{c}$, $b\left(\frac{t}{t_H(\kappa,k)}\right) \to 0$,
- if $t \ll \frac{|V|\kappa^2}{c}$, $b\left(\frac{t}{t_H(\kappa,k)}\right) \to 1$.

Consequently, because we aim at the largest generality possible, the term $b\left(\frac{t}{t_H(\kappa,k)}\right)$ in Eq. (30) must be kept as it is, without making any further simplification.

3.2.4. Multiple-path (pseudo-)correlation functions

Real Robin Laplacian. In Sec. 3.2.2, we mentioned that the universal correlation function was proved inaccurate when the positions $\boldsymbol{x}_1$ and $\boldsymbol{x}_2$ get close to the boundary surface. To address this issue, a general, system-dependent, non-stationary correlation function that is accurate even near the boundary surface was introduced in Hortikar and Srednicki (1998, Eq. (17)). This *multiple-path correlation function* is defined as a sum over all possible classical trajectories from $\boldsymbol{x}_1$ to $\boldsymbol{x}_2$ in the billiard, including the direct path:

$$C(\boldsymbol{x}_1, \boldsymbol{x}_2, \kappa, k) = \sum_p \epsilon^{r_p} \operatorname{sinc}(2\pi\kappa L_p(\boldsymbol{x}_1, \boldsymbol{x}_2)), \tag{32}$$

where:

- $\epsilon = 1$ for Neuman's boundary condition ($\widehat{\beta} = 0$), and $\epsilon = -1$ for Dirichlet's boundary condition ($\mathrm{Im}(\widehat{\beta}) \to -\infty$);
- r_p is the number of reflections along the p-th trajectory;
- L_p is the length of the p-th trajectory; for the direct path ($p = 0$), $L_0(\boldsymbol{x}_1, \boldsymbol{x}_2) = \|\boldsymbol{x}_1 - \boldsymbol{x}_2\|_2$, which corresponds to the universal correlation function introduced in Sec. 3.2.2.

In Eq. (32), the longer the trajectory, the lower the corresponding term, since its magnitude is proportional to $\frac{1}{L_p}$. In practice, the sum is finite because the discrete spectrum is smoothed over a bandwidth $\epsilon > 1/L_{\min}$, as explained at the end of Sec. 3.1.1 and at the beginning of Sec. 3.2. Finally, note that Eq. (32) also holds when the direct path between $\boldsymbol{x}_1$ and $\boldsymbol{x}_2$ is blocked by an obstacle. In such a case, the contribution of the universal correlation function in Eq. (32) is zero.

Complex Robin Laplacian. The general case of the complex Robin Laplacian was addressed in Badeau (2026d, Sec. IV D), and illustrated in Badeau (2026d, Fig. 1). Suppose that from position $\boldsymbol{x}_2 \in V$ to position $\boldsymbol{x}_1 \in V$, the p-th trajectory in the classical billiard undergoes r_p reflections on the boundary ∂V. For $q \in \{0 \dots r_p - 1\}$, the q-th reflection occurs at a reflection point $\boldsymbol{s}_{p,q} \in \partial V$, and is represented by a reflection matrix $\boldsymbol{R}_{p,q} \in \mathbb{R}^3$ w.r.t. the 2D subspace parallel to the plane tangent to ∂V at $\boldsymbol{s}_{p,q} \in \partial V$. Every reflection along trajectory p is mathematically described by a similarity transformation $\psi_{p,q}$, which assigns to any point $\boldsymbol{x} \in \mathbb{R}^3$ the point $\psi_{p,q}(\boldsymbol{x}) = \boldsymbol{s}_{p,q} + \boldsymbol{R}_{p,q}(\boldsymbol{x} - \boldsymbol{s}_{p,q})$. The composition of all successive reflections along the trajectory is also a similarity transformation (Badeau, 2026d, Eq. (25)):

$$\psi_p \triangleq \psi_{p,r_p-1} \circ \dots \circ \psi_{p,0}(\boldsymbol{x}) = \boldsymbol{Q}_p \boldsymbol{x} + \boldsymbol{y}_p, \tag{33}$$

where $\boldsymbol{Q}_p$ is an orthogonal matrix defined as

$$\boldsymbol{Q}_p = \boldsymbol{R}_{p,r_p-1} \dots \boldsymbol{R}_{p,0} \tag{34}$$

if $r_p > 0$, or $\boldsymbol{Q}_p = \boldsymbol{I}$ if $r_p = 0$, and $\boldsymbol{y}_p$ was defined in Badeau (2026d, Eq. (27)):

$$\begin{aligned} \boldsymbol{y}_p = & \left(\boldsymbol{I} - \boldsymbol{R}_{p,r_p-1}\right) \boldsymbol{s}_{p,r_p-1} \\ & + \sum_{q=0}^{r_p-2} \boldsymbol{R}_{p,r_p-1} \dots \boldsymbol{R}_{p,q+1} \left(\boldsymbol{I} - \boldsymbol{R}_{p,q}\right) \boldsymbol{s}_{p,q} \\ = & \sum_{q=0}^{r_p-1} \boldsymbol{R}_{p,r_p-1} \dots \boldsymbol{R}_{p,q+1} \left(\boldsymbol{I} - \boldsymbol{R}_{p,q}\right) \boldsymbol{s}_{p,q}, \end{aligned} \tag{35}$$

with the convention $\boldsymbol{R}_{p,r_p-1} \dots \boldsymbol{R}_{p,q+1} = \boldsymbol{I}$ for $q = r_p - 1$. Finally, the total length of trajectory p is (Badeau, 2026d, Eq. (29)):

$$L_p(\boldsymbol{x}_1, \boldsymbol{x}_2) = \left\|\boldsymbol{x}_1 - \psi_p(\boldsymbol{x}_2)\right\|_2, \tag{36}$$

where $\psi_p(\boldsymbol{x}_2)$ is the *image* of $\boldsymbol{x}_2$ through the composition of all reflections ψ_p. In Badeau (2026d, Eq. (34)), the *multiple-path pseudo-correlation function* $C(\boldsymbol{x}_1, \boldsymbol{x}_2, \mathcal{K}(K,k), k)$ that was introduced in Eq. (25) was then expressed as:

$$\begin{aligned} C(\boldsymbol{x}_1, \boldsymbol{x}_2, \kappa, k) = & \sum_p \tfrac{1}{4\pi} \int_{\boldsymbol{u} \in \mathcal{S}(0,1)} \left(\prod_{q=0}^{r_p-1} \tfrac{\kappa \boldsymbol{u}^\top \boldsymbol{R}_{p,r_p-1} \dots \boldsymbol{R}_{p,q+1} \boldsymbol{n}(\boldsymbol{s}_{p,q}) - k\widehat{\beta}(\boldsymbol{s}_{p,q},k)}{\kappa \boldsymbol{u}^\top \boldsymbol{R}_{p,r_p-1} \dots \boldsymbol{R}_{p,q+1} \boldsymbol{n}(\boldsymbol{s}_{p,q}) + k\widehat{\beta}(\boldsymbol{s}_{p,q},k)} \right) \\ & \times \tfrac{e^{\imath 2\pi\kappa \boldsymbol{u}^\top (\boldsymbol{x}_1 - \boldsymbol{Q}_p \boldsymbol{x}_2 - \boldsymbol{y}_p)} + e^{\imath 2\pi\kappa \boldsymbol{u}^\top (\boldsymbol{x}_2 - \boldsymbol{Q}_p \boldsymbol{x}_1 - \boldsymbol{y}_p)}}{2} dS(\boldsymbol{u}). \end{aligned} \tag{37}$$

In the Neumann case ($\epsilon = 1$) and in the Dirichlet case ($\epsilon = -1$), Eq. (37) reduces to Eq. (32).

In addition, in Badeau (2026d, Eq. (36)), the *multiple-path correlation function* γ that was introduced in Eq. (24) was expressed as:

$$\gamma(\boldsymbol{x}_1, \boldsymbol{x}_2, K, k_1, k_2) = \tfrac{\mathring{\gamma}(\boldsymbol{x}_1, \boldsymbol{x}_2, K, k_1, k_2) + \overline{\mathring{\gamma}(\boldsymbol{x}_2, \boldsymbol{x}_1, K, k_2, k_1)}}{2}, \tag{38}$$

with (Badeau, 2026d, Eq. (37)):

$$\begin{aligned} \mathring{\gamma}(\boldsymbol{x}_1, \boldsymbol{x}_2, K, k_1, k_2) = & \sum_p \tfrac{1}{4\pi} \int_{\boldsymbol{u} \in \mathcal{S}(0,1)} e^{\imath 2\pi \boldsymbol{u}^\top \left(\mathcal{K}(K,k_1)\boldsymbol{x}_1 - \overline{\mathcal{K}(K,k_2)} \boldsymbol{Q}_p \boldsymbol{x}_2 - K \boldsymbol{y}_p\right)} \\ & \times e^{\imath \left(\theta(\boldsymbol{u},K,k_1) - \overline{\theta\left(\boldsymbol{Q}_p^\top \boldsymbol{u}, K, k_2\right)}\right)} dS(\boldsymbol{u}), \end{aligned} \tag{39}$$

where the phase distortion $\theta(\boldsymbol{u}, K, k)$ was defined in Eq. (29).

3.3. Consistency betweeen the eigenspectrum model and the random wave model

To summarize the discussion in Sec. 3.2, we will consider in this paper a Gaussian model of the eigenfunctions, involving either the universal (pseudo-)correlation functions introduced in Sec. 3.2.2, or the more accurate multiple-path (pseudo-)correlation functions presented in Sec. 3.2.4. In Sec. 4, the GOE probabilistic model of the eigenspectrum introduced in Sec. 3.1.3 will be combined with one of the two kinds of correlation functions, in order to determine the first and second order statistics of the RIR.

However, there is one pitfall we must avoid. If we consider the universal (pseudo-)correlation functions introduced in Sec. 3.2.2, then the GOE model of the eigenspectrum must involve the asymptotic expansion of the modal density described in Eq. (13). Indeed, if we compare the Neumann and Dirichlet boundary conditions for instance, then it is well known that the power of the eigenfunctions is zero at the boundary in the Dirichlet case, whereas it is twice the average power in the interior of the room in the Neumann case. In other respects, because the eigenfunctions are modeled as stationary, independent, and carry on average the same quantity of power as shown in Eq. (27), the power spectral density (PSD) of the wave field is proportional to the smoothed modal density, as explained e.g. in Badeau (2024, Sec. I) and expressed in Eq. (64). As this PSD corresponds to an average power over *space* (which combines with the spectral averaging described at the beginning of Sec. 3.2) that includes the vicinity of the boundary, then it must be slightly greater in the Neumann case than in the Dirichlet case. And indeed, the first order surface term of the modal density in Eq. (13), which reflects the boundary condition and accounts for the first order reflections, is positive in the Neumann case, whereas it is negative in the Dirichlet case.

However, the situation is different if we consider the multiple-path (pseudo-)correlation functions presented in Sec. 3.2.4: in this case, all the reflections are directly taken into account in the eigenfunction model. In particular, Eq. (32) innately accounts for the doubling of the eigenfunctions' power at the boundary in the Neumann case, and for their zeroing in the Dirichlet case. Therefore, the reflections *must not* be taken into account in the expression of the modal density, otherwise their contribution to the power of the RIR would be counted twice. For this reason, the first order surface term must be removed from the modal density when the multiple-path correlation function is considered or, in other words, the original Weyl formula [Eq. (12)] should be used instead of Eq. (13). This change calls for a comment: of course, the accurate modal density is always given by Eq. (13), independently of the RWM chosen. However, the multiple-path correlation function corresponds to a slightly different definition of spectral averaging: in Eqs. (22) and (23) for instance, function $\rho(\kappa, k)$ in the denominator is defined by Eq. (12) instead of Eq. (13).

3.4. Cross-Wigner time-frequency distribution

When there is energy absorption at the domain's boundary, the RIR $h(\boldsymbol{x}^r, \boldsymbol{x}^s, t)$ defined in Sec. 2.1 is modeled as a non-stationary random process, due to the exponential damping of the eigenmodes over time. In signal processing, the standard tool for characterizing the second-order statistics of a non-stationary random process is the *Wigner distribution* (Cohen, 1989), also known as the Wigner-Ville distribution, which describes how the power of this random process is distributed in the time-frequency plane. Let

$$\Gamma_h(\boldsymbol{x}_1^r, \boldsymbol{x}_1^s, \boldsymbol{x}_2^r, \boldsymbol{x}_2^s, t_1, t_2) = \operatorname{cov}[h(\boldsymbol{x}_1^r, \boldsymbol{x}_1^s, t_1), h(\boldsymbol{x}_2^r, \boldsymbol{x}_2^s, t_2)] \tag{40}$$

denote the *auto-covariance function* (ACF) of the non-stationary random process $h(\boldsymbol{x}^r, \boldsymbol{x}^s, t)$, where $\boldsymbol{x}^r, \boldsymbol{x}^s \in V$ and $t \in \mathbb{R}$. Its *cross-Wigner distribution* W_h is then defined as follows: $\forall \boldsymbol{x}_1^r, \boldsymbol{x}_1^s, \boldsymbol{x}_2^r, \boldsymbol{x}_2^s \in V$, $\forall f, t \in \mathbb{R}$,

$$W_h(\boldsymbol{x}_1^r, \boldsymbol{x}_1^s, \boldsymbol{x}_2^r, \boldsymbol{x}_2^s, f, t) = \int_{\mathbb{R}} \Gamma_h(\boldsymbol{x}_1^r, \boldsymbol{x}_1^s, \boldsymbol{x}_2^r, \boldsymbol{x}_2^s, t + \tfrac{\tau}{2}, t - \tfrac{\tau}{2})\, e^{-2\imath\pi f \tau} d\tau. \tag{41}$$

The cross-Wigner distribution W_h in Eq. (41) can be interpreted as the covariance of the random process h between two receiver positions $\boldsymbol{x}_1^r$ and $\boldsymbol{x}_2^r$, and two source positions $\boldsymbol{x}_1^s$ and $\boldsymbol{x}_2^s$, at frequency f and time t. In Sec. 4.3.3, $W_h(\boldsymbol{x}_1^r, \boldsymbol{x}_1^s, \boldsymbol{x}_2^r, \boldsymbol{x}_2^s, f, t)$ will be calculated in closed form.

4. First and second-order wave field statistics

In this section, the first and second-order wave field statistics are investigated, based on the probabilistic model of the eigenspectrum presented in Sec. 3.1, and on the RWM of the eigenfunctions introduced in Badeau (2026d, Sec. IV). The same method as in our previous papers on the statistical wave field theory is used here: from the statistics of the B-function (Sec. 4.1), the statistics of the Green's function of the Helmholtz equation are derived (Sec. 4.2), from which the statistics of the room impulse response are finally deduced (Sec. 4.3).

4.1. B-function

Let us first recall the expression of the B-function, which was introduced in Sec. 2.3, in a bounded domain V (Badeau, 2024, Eq. (38)):

$$B(\boldsymbol{y}^r, \boldsymbol{x}^s, k) = \sum_{n \in \mathbb{N}} \varphi_n(\boldsymbol{y}^r, k)\, \varphi_n(\boldsymbol{x}^s, k). \tag{42}$$

In this expression, remember that the image source position $\boldsymbol{y}^r$ is not restricted to the room's space: it can be anywhere in $\mathbb{R}^3$.

Before we begin, let us make an important remark: it is well known that the restriction of the series in Eq. (42) to the domain V converges to the Dirac delta function $\delta(\boldsymbol{y}^r - \boldsymbol{x}^s)$ when the Laplace operator $-\Delta$ is self-adjoint, i.e., when there is no energy absorption. However, the convergence of series involving the eigenfunctions of a linear operator, such as that in Eq. (42), is generally not guaranteed when this operator is not self-adjoint (Badeau, 2025a). And indeed, when $\widehat{\beta}$ is not purely imaginary, the complex Laplace operator is not self-adjoint, as already mentioned in Sec. 2.4. However, we will prove in Appendix A.1 that when the eigenfunctions φ_n follow the RWM described in Badeau (2026d, Sec. IV), then for any source position $\boldsymbol{x}^s \in V$, the series in Eq. (42) converges almost surely to a distribution w.r.t. $\boldsymbol{y}^r \in \mathbb{R}^3$, so this expression does make sense mathematically. In this section, in order to keep the mathematical developments as simple as possible, we will continue writing equations such as Eq. (42) without taking care of the convergence of the series, but the reader should be aware that a more rigorous mathematical treatment would require applying the B-function against smooth functions with compact support in all equations, as done in Appendix A.1.

4.1.1. Mathematical expectation of the B-function

Let us first calculate the mathematical expectation of the B-function when the wave numbers are fixed, i.e., when the measure μ introduced in Eq. (16) is deterministic, and only the eigenfunctions φ_n are random. Applying the mathematical expectation w.r.t φ_n to Eq. (42) yields

$$\begin{aligned}\mathbb{E}[B(\boldsymbol{y}^r, \boldsymbol{x}^s, k)] = & \ \lambda \sum_{n\in\mathbb{N}} C(\boldsymbol{y}^r, \boldsymbol{x}^s, \mathcal{K}(K_n, k), k) \\ = & \ \lambda \int_{K\in\mathbb{R}_+} C(\boldsymbol{y}^r, \boldsymbol{x}^s, \mathcal{K}(K, k), k) d\mu(K, 0),\end{aligned}$$

where we have successively substituted Eqs. (25) and (16). Then, by applying the mathematical expectation w.r.t the random measure μ, we get

$$\mathbb{E}[B(\boldsymbol{y}^r, \boldsymbol{x}^s, k)] = \lambda \int_{K\in\mathbb{R}_+} C(\boldsymbol{y}^r, \boldsymbol{x}^s, \mathcal{K}(K, k), k) \rho(K, 0) dK, \tag{43}$$

where we have used Eq. (17). Then, by substituting Eq. (14) and by applying the change of variable $\kappa = \mathcal{K}(K, k)$, we get

$$\begin{aligned}\mathbb{E}[B(\boldsymbol{y}^r, \boldsymbol{x}^s, k)] = & \ \lambda \int_{K\in\mathbb{R}_+} C(\boldsymbol{y}^r, \boldsymbol{x}^s, \mathcal{K}(K, k), k) \\ & \times \rho(\mathcal{K}(K, k), k) \frac{\partial \mathcal{K}(K,k)}{\partial K} dK \\ = & \ \lambda \int_{\kappa\in\mathcal{K}(\mathbb{R}_+, k)} C(\boldsymbol{y}^r, \boldsymbol{x}^s, \kappa, k) \rho(\kappa, k) d\kappa \\ = & \ \lambda \int_{\kappa\in\mathbb{R}_+} C(\boldsymbol{y}^r, \boldsymbol{x}^s, \kappa, k) \rho(\kappa, k) d\kappa,\end{aligned} \tag{44}$$

where the last equality is obtained by applying Cauchy's integral theorem. Now, let us focus on two particular cases: the Neumann ($\epsilon = 1$) and Dirichlet ($\epsilon = -1$) boundary conditions. Then, if we consider the multiple-path pseudo-correlation function in Eq. (32) along with the modal density in Eq. (12), as explained in Sec. 3.3, Eq. (44) yields:

$$\mathbb{E}[B(\boldsymbol{y}^r, \boldsymbol{x}^s, k)] = 4\pi \sum_p \epsilon^{r_p} \int_{\kappa\in\mathbb{R}_+} \operatorname{sinc}\left(2\pi\kappa \left\|\boldsymbol{y}^r - \psi_p(\boldsymbol{x}^s)\right\|_2\right) \kappa^2 d\kappa,$$

where ψ_p is the similarity transformation defined in Eq. (33), and $\psi_p(\boldsymbol{x}^s)$ is the image of the source that corresponds to the p-th trajectory in the classical billiard. Finally, the integral over κ can be calculated in closed form:

$$\mathbb{E}[B(\boldsymbol{y}^r, \boldsymbol{x}^s, k)] = \sum_p \epsilon^{r_p} \, \delta\left(\boldsymbol{y}^r - \psi_p(\boldsymbol{x}^s)\right). \tag{45}$$

We thus obtain a remarkable result: the mean of the B-function matches exactly the spatial distribution of the first image sources as predicted by geometrical acoustics (remember that the sum in Eq. (45) is finite due to spectral smoothing, as explained in Sec. 3.2.4). In other words, the prediction of early echos is retrieved in the first order statistics of the B-function.

Of course, this result also holds in the general case of the complex Robin boundary condition with an arbitrary number of reflections, even though in this case we do not get a closed-form expression as simple as that in Eq. (45). Nevertheless, this can be easily shown if we consider the multiple-path pseudo-correlation function in Eq. (37), restricted to the direct path ($p = 0$, $r_p = 0$, $\boldsymbol{Q}_p = \boldsymbol{I}$), assuming that this path is not blocked by an obstacle, and to the first order reflections ($p > 0$, $r_p = 1$, $\boldsymbol{Q}_p = \boldsymbol{R}_{p,0}$). Then, substituting Eqs. (37) and (12) into Eq. (44) yields:

$$\begin{aligned}
\mathbb{E}[B(\boldsymbol{y}^r, \boldsymbol{x}^s, k)] = & \int_{\kappa\in\mathbb{R}_+} \int_{\boldsymbol{u}\in\mathcal{S}(0,1)} \\
& \Big(e^{\imath 2\pi\kappa\boldsymbol{u}^\top(\boldsymbol{y}^r-\boldsymbol{x}^s)} + \sum_{p>0} \tfrac{\kappa\boldsymbol{u}^\top\boldsymbol{n}(\boldsymbol{s}_{p,0})-k\widehat{\beta}(\boldsymbol{s}_{p,0},k)}{\kappa\boldsymbol{u}^\top\boldsymbol{n}(\boldsymbol{s}_{p,0})+k\widehat{\beta}(\boldsymbol{s}_{p,0},k)} \\
& \times e^{\imath 2\pi\kappa\boldsymbol{u}^\top(\boldsymbol{y}^r-\boldsymbol{R}_{p,0}\boldsymbol{x}^s-\boldsymbol{y}_p)}\Big) dS(\boldsymbol{u})\, \kappa^2 d\kappa \\
= & \int_{\boldsymbol{\kappa}\in\mathbb{R}^3} \Big(e^{-\imath 2\pi\boldsymbol{\kappa}^\top\boldsymbol{x}^s} + \sum_{p>0} \tfrac{\boldsymbol{\kappa}^\top\boldsymbol{n}(\boldsymbol{s}_{p,0})-k\widehat{\beta}(\boldsymbol{s}_{p,0},k)}{\boldsymbol{\kappa}^\top\boldsymbol{n}(\boldsymbol{s}_{p,0})+k\widehat{\beta}(\boldsymbol{s}_{p,0},k)} \\
& \times e^{-\imath 2\pi\boldsymbol{\kappa}^\top(\boldsymbol{R}_{p,0}\boldsymbol{x}^s+\boldsymbol{y}_p)}\Big) e^{\imath 2\pi\boldsymbol{\kappa}^\top\boldsymbol{y}^r} d\boldsymbol{\kappa},
\end{aligned}$$

where the first equality is obtained by noticing that for $r_p = 1$, Eq. (35) yields $-\boldsymbol{R}_{p,0}\,\boldsymbol{y}_p = \boldsymbol{y}_p$, and the second equality is obtained by applying the change of variable $\boldsymbol{\kappa} = \kappa\boldsymbol{u}$, which is such that $d\boldsymbol{\kappa} = \kappa^2 d\kappa dS(\boldsymbol{u})$. From this equation, we immediately deduce that the 3D Fourier transform of the B-function w.r.t. $\boldsymbol{y}^r$ is such that

$$\mathbb{E}[\widehat{B}(\boldsymbol{\kappa}, \boldsymbol{x}^s, k)] = e^{-\imath 2\pi\boldsymbol{\kappa}^\top\boldsymbol{x}^s} + \sum_{p>0} \tfrac{\boldsymbol{\kappa}^\top\boldsymbol{n}(\boldsymbol{s}_{p,0})-k\widehat{\beta}(\boldsymbol{s}_{p,0},k)}{\boldsymbol{\kappa}^\top\boldsymbol{n}(\boldsymbol{s}_{p,0})+k\widehat{\beta}(\boldsymbol{s}_{p,0},k)} e^{-\imath 2\pi\boldsymbol{\kappa}^\top(\boldsymbol{R}_{p,0}\boldsymbol{x}^s+\boldsymbol{y}_p)}.$$

We thus retrieve exactly the same terms as in Badeau (2024, Eq. (30)), which shows that the mean of the B-function matches exactly the spatial distribution of the original source, and of the first order image sources w.r.t. the complex impedance planes tangent to the boundary surface at the reflection points $\boldsymbol{s}_{p,0}$.

Alternatively, if we focus again on the Neumann ($\epsilon = 1$) and Dirichlet ($\epsilon = -1$) boundary conditions, and if we now consider the universal pseudo-correlation function in Eq. (26) along with the modal density in Eq. (13), as explained in Sec. 3.3, then Eq. (44) yields:

$$\mathbb{E}[B(\boldsymbol{y}^r, \boldsymbol{x}^s, k)] = 4\pi \int_{\kappa\in\mathbb{R}_+} \mathrm{sinc}\left(2\pi\kappa\|\boldsymbol{y}^r - \boldsymbol{x}^s\|_2\right) \left(\kappa^2 + \epsilon\tfrac{\lambda S(\partial V)}{8}\kappa\right) d\kappa.$$

Again, the integral over κ can be calculated in closed form:

$$\mathbb{E}[B(\boldsymbol{y}^r, \boldsymbol{x}^s, k)] = \delta(\boldsymbol{y}^r - \boldsymbol{x}^s) + \epsilon\,\tfrac{\lambda S(\partial V)}{8\pi\|\boldsymbol{y}^r-\boldsymbol{x}^s\|_2^2}. \tag{46}$$

In the right member of Eq. (46), the first term is a Dirac at the original source position, as in Eq. (45) for $p = 0$ (assuming that the direct path is not blocked by an obstacle). The second term is a universal surface term, which is an average of the spatial distribution of all possible first order image sources, when the room's geometry is unknown. This term is slowly varying and non-oscillating, thus negligible at high frequency.

4.1.2. Second order moments

Now, let us calculate the second order moments of the B-function when the wave numbers are fixed, i.e., when the measure μ is deterministic, and only the eigenfunctions φ_n are random. By substituting Eq. (42), applying Lemma 1, and finally substituting Eqs. (24) and (25), we get

$$\begin{aligned}
& \mathbb{E}[B(\boldsymbol{y}_1^r,\boldsymbol{x}_1^s,k_1)\,\overline{B(\boldsymbol{y}_2^r,\boldsymbol{x}_2^s,k_2)}] \\
= \; & \lambda^2 \sum_{n\in\mathbb{N}} \Big(\gamma(\boldsymbol{y}_1^r,\boldsymbol{y}_2^r,K_n,k_1,k_2)\,\gamma(\boldsymbol{x}_1^s,\boldsymbol{x}_2^s,K_n,k_1,k_2) \\
& +\gamma(\boldsymbol{y}_1^r,\boldsymbol{x}_2^s,K_n,k_1,k_2)\,\gamma(\boldsymbol{x}_1^s,\boldsymbol{y}_2^r,K_n,k_1,k_2)\Big) \\
& +\lambda^2 \sum_{n_1\in\mathbb{N}} C(\boldsymbol{y}_1^r,\boldsymbol{x}_1^s,\mathcal{K}(K_{n_1},k_1),k_1) \\
& \times \sum_{n_2\in\mathbb{N}} \overline{C(\boldsymbol{y}_2^r,\boldsymbol{x}_2^s,\mathcal{K}(K_{n_2},k_2),k_2)} \\
= \; & \lambda^2 \int_{K\in\mathbb{R}_+} \Big(\gamma(\boldsymbol{y}_1^r,\boldsymbol{y}_2^r,K,k_1,k_2)\,\gamma(\boldsymbol{x}_1^s,\boldsymbol{x}_2^s,K,k_1,k_2) \\
& +\gamma(\boldsymbol{y}_1^r,\boldsymbol{x}_2^s,K,k_1,k_2)\,\gamma(\boldsymbol{x}_1^s,\boldsymbol{y}_2^r,K,k_1,k_2)\Big) d\mu(K,0) \\
& +\lambda^2 \int_{K_1\in\mathbb{R}_+} C(\boldsymbol{y}_1^r,\boldsymbol{x}_1^s,\mathcal{K}(K_1,k_1),k_1) d\mu(K_1,0) \\
& \times \int_{K_2\in\mathbb{R}_+} \overline{C(\boldsymbol{y}_2^r,\boldsymbol{x}_2^s,\mathcal{K}(K_2,k_2),k_2)} d\mu(K_2,0),
\end{aligned}$$

where we have substituted Eq. (16) in the last equality. Then, by applying the mathematical expectation w.r.t. the random measure μ, we get

$$\begin{aligned}
& \mathbb{E}[B(\boldsymbol{y}_1^r,\boldsymbol{x}_1^s,k_1)\,\overline{B(\boldsymbol{y}_2^r,\boldsymbol{x}_2^s,k_2)}] \\
= \; & \lambda^2 \int_{K\in\mathbb{R}_+} \Big(\gamma(\boldsymbol{y}_1^r,\boldsymbol{y}_2^r,K,k_1,k_2)\gamma(\boldsymbol{x}_1^s,\boldsymbol{x}_2^s,K,k_1,k_2) \\
& +\gamma(\boldsymbol{y}_1^r,\boldsymbol{x}_2^s,K,k_1,k_2)\gamma(\boldsymbol{x}_1^s,\boldsymbol{y}_2^r,K,k_1,k_2)\Big)\rho(K,0)dK \\
& +\lambda^2 \iint_{K_1,K_2\in\mathbb{R}_+} C(\boldsymbol{y}_1^r,\boldsymbol{x}_1^s,\mathcal{K}(K_1,k_1),k_1) \\
& \times\overline{C(\boldsymbol{y}_2^r,\boldsymbol{x}_2^s,\mathcal{K}(K_2,k_2),k_2)}\,\rho\,(K_1,0)\,\rho\,(K_2,0) \\
& \times R_2\left((K_1-K_2)\rho\left(\tfrac{K_1+K_2}{2},0\right)\right) dK_1 dK_2,
\end{aligned} \tag{47}$$

where we have used Eqs. (17) and (18). With the same change of variable $K_1 = K + \frac{s}{2\rho(K,0)}$ and $K_2 = K - \frac{s}{2\rho(K,0)}$ as in Sec. 3.1.3, we get asymptotically

$$\begin{aligned}
& \mathbb{E}[B(\boldsymbol{y}_1^r,\boldsymbol{x}_1^s,k_1)\,\overline{B(\boldsymbol{y}_2^r,\boldsymbol{x}_2^s,k_2)}] \\
= \; & \lambda^2 \int_{K\in\mathbb{R}_+} \Big(\gamma(\boldsymbol{y}_1^r,\boldsymbol{y}_2^r,K,k_1,k_2)\,\gamma(\boldsymbol{x}_1^s,\boldsymbol{x}_2^s,K,k_1,k_2) \\
& +\gamma(\boldsymbol{y}_1^r,\boldsymbol{x}_2^s,K,k_1,k_2)\,\gamma(\boldsymbol{x}_1^s,\boldsymbol{y}_2^r,K,k_1,k_2) \\
& +\int_{s\in\mathbb{R}} C(\boldsymbol{y}_1^r,\boldsymbol{x}_1^s,\mathcal{K}(K+\tfrac{s}{2\rho(K,0)},k_1),k_1) \\
& \times\overline{C(\boldsymbol{y}_2^r,\boldsymbol{x}_2^s,\mathcal{K}(K-\tfrac{s}{2\rho(K,0)},k_2),k_2)}(1-Y(s))\,ds\Big) \\
& \rho(K,0)dK,
\end{aligned} \tag{48}$$

where the level cluster function $Y(s)$ was defined in Eq. (20).

4.2. Green's function of the Helmholtz equation

Thanks to Eq. (8), the first and second order statistics of the Green's function $G(\boldsymbol{x}^r, \boldsymbol{x}^s, k)$ can be directly derived from those of the B-function, which were calculated in Sec. 4.1.

4.2.1. Mathematical expectation

The mathematical expectation of $G(\boldsymbol{x}^r, \boldsymbol{x}^s, k)$ can be deduced from that of the B-function, by solving the partial differential equation (PDE)

$$-(\Delta_{\boldsymbol{y}^r} + 4\pi^2 k^2)\mathbb{E}[G(\boldsymbol{y}^r, \boldsymbol{x}^s, k)] = \mathbb{E}[B(\boldsymbol{y}^r, \boldsymbol{x}^s, k)], \tag{49}$$

which follows from Eq. (8). Indeed, given that both expressions of the pseudo-correlation function $C(\boldsymbol{x}_1, \boldsymbol{x}_2, \kappa, k)$ in Eqs. (26) and (37) satisfy $\Delta_{\boldsymbol{x}_1} C(\boldsymbol{x}_1, \boldsymbol{x}_2, \kappa, k) = -4\pi^2\kappa^2 C(\boldsymbol{x}_1, \boldsymbol{x}_2, \kappa, k)$, the following formula

$$\mathbb{E}[G(\boldsymbol{x}^r, \boldsymbol{x}^s, k)] = \frac{\lambda}{4\pi^2}\int_{\kappa\in\mathbb{R}_+} \frac{C(\boldsymbol{x}^r,\boldsymbol{x}^s,\kappa,k)}{\kappa^2-k^2}\rho(\kappa, k)d\kappa \tag{50}$$

does provide a solution to Eq. (49), where $\mathbb{E}[B(\boldsymbol{y}^r, \boldsymbol{x}^s, k)]$ was expressed in Eq. (44).

Now, let us focus on two particular cases: the Neumann ($\epsilon = 1$) and Dirichlet ($\epsilon = -1$) boundary conditions. Then, if we consider the multiple-path pseudo-correlation function in Eq. (32) along with the modal density in Eq. (12), as explained in Sec. 3.3, the integral in Eq. (50) can be calculated in closed-form by using the residue theorem[1] (Ahlfors, 1979):

$$\begin{aligned}\mathbb{E}[G(\boldsymbol{x}^r, \boldsymbol{x}^s, k)] &= \sum_p \epsilon^{r_p} \frac{\cos(2\pi k\|\boldsymbol{x}^r - (\boldsymbol{Q}_p\boldsymbol{x}^s + \boldsymbol{y}_p)\|_2)}{4\pi\|\boldsymbol{x}^r - (\boldsymbol{Q}_p\boldsymbol{x}^s + \boldsymbol{y}_p)\|_2}\\ &= \sum_p \epsilon^{r_p} G_0\left(\boldsymbol{x}^r - \psi_p(\boldsymbol{x}^s), k\right),\end{aligned}$$

where function $G_0(\boldsymbol{z}, k)$ is the free field Green's function defined in Eq. (7), and ψ_p is the similarity transformation defined in Eq. (33).

Alternatively, if we consider the universal pseudo-correlation function in Eq. (26) along with the modal density in Eq. (13), as explained in Sec. 3.3, the expectation of the B-function was expressed in Eq. (46). From this equation, solving the PDE in Eq. (49) leads to

$$\begin{aligned}\mathbb{E}[G(\boldsymbol{x}^r, \boldsymbol{x}^s, k)] = &\frac{\cos(2\pi k\|\boldsymbol{x}^r-\boldsymbol{x}^s\|_2)\left(1+\frac{\epsilon\lambda S(\partial V)\mathrm{Si}(2\pi k\|\boldsymbol{x}^r-\boldsymbol{x}^s\|_2)}{4\pi k}\right)}{4\pi\|\boldsymbol{x}^r-\boldsymbol{x}^s\|_2}\\ &-\frac{\sin(2\pi k\|\boldsymbol{x}^r-\boldsymbol{x}^s\|_2)\frac{\epsilon\lambda S(\partial V)\mathrm{Ci}(2\pi|k|\|\boldsymbol{x}^r-\boldsymbol{x}^s\|_2)}{4\pi k}}{4\pi\|\boldsymbol{x}^r-\boldsymbol{x}^s\|_2},\end{aligned} \tag{51}$$

where $\mathrm{Ci}(x)$ is the *cosine integral* function: $\mathrm{Ci}(x) = -\int_x^{+\infty}\frac{\cos(u)}{u}du$, and $\mathrm{Si}(x)$ is the *sine integral* function: $\mathrm{Si}(x) = \int_0^x \frac{\sin(u)}{u}du$. The mathematical derivations that lead to Eq. (51) from Eqs. (49) and (46) are lengthy and are thus omitted here, but conversely, it is easy to verify that the function $\mathbb{E}[G(\boldsymbol{x}^r, \boldsymbol{x}^s, k)]$ defined in Eq. (51) is indeed a solution to Eq. (49), with $\mathbb{E}[B(\boldsymbol{y}^r, \boldsymbol{x}^s, k)]$ expressed as in Eq. (46).

---

[1] We can choose two integration contours that contain an interval of $\mathbb{R}$ centered at $\kappa = 0$, given that the integrand in the right member of Eq. (50) is an even function of κ, one contour in the upper half complex plane, and the other in the lower half complex plane. Moreover, the denominator contains two real poles at $\kappa = k$ and $\kappa = -k$, which belong to these two contours, so the corresponding residues are divided by two.

4.2.2. Second order moments

In the same way, the second order moments of $G(\boldsymbol{x}^r, \boldsymbol{x}^s, k)$ can be deduced from those of the B-function, by solving the following PDE:

$$\begin{aligned} & (\Delta_{\boldsymbol{y}_1^r} + 4\pi^2 k_1^2)\overline{(\Delta_{\boldsymbol{y}_2^r} + 4\pi^2 k_2^2)}\mathbb{E}[G(\boldsymbol{y}_1^r, \boldsymbol{x}_1^s, k_1)\,\overline{G(\boldsymbol{y}_2^r, \boldsymbol{x}_2^s, k_2)}] \\ = \ & \mathbb{E}[B(\boldsymbol{y}_1^r, \boldsymbol{x}_1^s, k_1)\,\overline{B(\boldsymbol{y}_2^r, \boldsymbol{x}_2^s, k_2)}], \end{aligned} \tag{52}$$

which follows from Eq. (8). Indeed, given that both expressions of the pseudo-correlation function $C(\boldsymbol{x}_1, \boldsymbol{x}_2, \kappa, k)$ in Eqs. (26) and (37) satisfy

$$\Delta_{\boldsymbol{x}_1} C(\boldsymbol{x}_1, \boldsymbol{x}_2, \kappa, k) = -4\pi^2\kappa^2 C(\boldsymbol{x}_1, \boldsymbol{x}_2, \kappa, k),$$

and both expressions of the correlation function $\gamma(\boldsymbol{x}_1, \boldsymbol{x}_2, K, k_1, k_2)$ in Eqs. (28) and (38) satisfy

$$\Delta_{\boldsymbol{x}_1}\gamma(\boldsymbol{x}_1, \boldsymbol{x}_2, K, k_1, k_2) = -4\pi^2\mathcal{K}(K, k_1)^2\gamma(\boldsymbol{x}_1, \boldsymbol{x}_2, K, k_1, k_2)$$

and

$$\Delta_{\boldsymbol{x}_2}\gamma(\boldsymbol{x}_1, \boldsymbol{x}_2, K, k_1, k_2) = -4\pi^2\overline{\mathcal{K}(K, k_2)^2}\gamma(\boldsymbol{x}_1, \boldsymbol{x}_2, K, k_1, k_2),$$

the following formula

$$\begin{aligned} & \mathbb{E}[G(\boldsymbol{x}_1^r, \boldsymbol{x}_1^s, k_1)\,\overline{G(\boldsymbol{x}_2^r, \boldsymbol{x}_2^s, k_2)}] \\ = \ & \tfrac{\lambda^2}{16\pi^4}\int_{K\in\mathbb{R}_+}\Big(\tfrac{\gamma(\boldsymbol{x}_1^r, \boldsymbol{x}_2^r, K, k_1, k_2)\,\gamma(\boldsymbol{x}_1^s, \boldsymbol{x}_2^s, K, k_1, k_2)}{\left(\mathcal{K}(K,k_1)^2 - k_1^2\right)\overline{\left(\mathcal{K}(K,k_2)^2 - k_2^2\right)}} \\ & + \tfrac{\gamma(\boldsymbol{x}_1^r, \boldsymbol{x}_2^s, K, k_1, k_2)\,\gamma(\boldsymbol{x}_1^s, \boldsymbol{x}_2^r, K, k_1, k_2)}{\left(\mathcal{K}(K,k_1)^2 - k_1^2\right)\overline{\left(\mathcal{K}(K,k_2)^2 - k_2^2\right)}} \\ & + \int_{s\in\mathbb{R}} C(\boldsymbol{x}_1^r, \boldsymbol{x}_1^s, \mathcal{K}(K + \tfrac{s}{2\rho(K,0)}, k_1), k_1) \\ & \times\overline{C(\boldsymbol{x}_2^r, \boldsymbol{x}_2^s, \mathcal{K}(K - \tfrac{s}{2\rho(K,0)}, k_2), k_2)}\,\rho(K,0) \\ & \tfrac{1 - Y(s)}{\left(\mathcal{K}(K + \frac{s}{2\rho(K,0)}, k_1)^2 - k_1^2\right)\overline{\left(\mathcal{K}(K - \frac{s}{2\rho(K,0)}, k_2)^2 - k_2^2\right)}}\,ds\Big)dK \end{aligned} \tag{53}$$

does provide a solution to Eq. (52), where $\mathbb{E}[B(\boldsymbol{y}_1^r, \boldsymbol{x}_1^s, k_1)\,\overline{B(\boldsymbol{y}_2^r, \boldsymbol{x}_2^s, k_2)}]$ was expressed in Eq. (48).

4.3. Room impulse response

Based on Eq. (6), the first and second order statistics of a solution $g(\boldsymbol{x}^r, \boldsymbol{x}^s, t)$ to the inhomogeneous wave equation [Eq. (3)] can be deduced from those of the Green's function $G(\boldsymbol{x}^r, \boldsymbol{x}^s, k)$, which were calculated in Sec. 4.2. The statistics of the causal RIR $h(\boldsymbol{x}^r, \boldsymbol{x}^s, t)$ can then be directly deduced from those of $g(\boldsymbol{x}^r, \boldsymbol{x}^s, t)$.

4.3.1. Mathematical expectation

By applying the mathematical expectation to Eq. (6), we first get

$$\mathbb{E}[g(\boldsymbol{x}^r, \boldsymbol{x}^s, t)] = \int_{f\in\mathbb{R}}\mathbb{E}[G(\boldsymbol{x}^r, \boldsymbol{x}^s, \tfrac{f}{c})]e^{\imath 2\pi f t}df. \tag{54}$$

Then, by substituting Eq. (50) into Eq. (54), we get

$$\mathbb{E}[g(\boldsymbol{x}^r, \boldsymbol{x}^s, t)] = -\frac{\lambda c^2}{4\pi^2} \int_{\kappa \in \mathbb{R}_+} \int_{f \in \mathbb{R}} \frac{C(\boldsymbol{x}^r, \boldsymbol{x}^s, \kappa, \frac{f}{c})}{f^2 - c^2\kappa^2} \rho(\kappa, \tfrac{f}{c}) e^{\imath 2\pi f t} df \, d\kappa. \tag{55}$$

By applying the residue theorem[2] (Ahlfors, 1979), we then get

$$\mathbb{E}[g(\boldsymbol{x}^r, \boldsymbol{x}^s, t)] = \frac{\lambda c}{4\pi} \operatorname{sign}(t) \operatorname{Im} \int_{\kappa \in \mathbb{R}_+} C(\boldsymbol{x}^r, \boldsymbol{x}^s, \kappa, \kappa) \frac{\rho(\kappa, \kappa)}{\kappa} e^{\imath 2\pi c \kappa t} d\kappa. \tag{56}$$

Now, let us focus on two particular cases: the Neumann ($\epsilon = 1$) and Dirichlet ($\epsilon = -1$) boundary conditions. Then, if we consider the multiple-path pseudo-correlation function in Eq. (32) along with the modal density in Eq. (12), as explained in Sec. 3.3, the integral in Eq. (56) can be calculated in closed-form:

$$\mathbb{E}[g(\boldsymbol{x}^r, \boldsymbol{x}^s, t)] = \frac{1}{8\pi L_p(\boldsymbol{x}^r, \boldsymbol{x}^s)} \operatorname{sign}(t) \sum_p \epsilon^{r_p} \left(\delta(t - \tfrac{L_p(\boldsymbol{x}^r, \boldsymbol{x}^s)}{c}) - \delta(t + \tfrac{L_p(\boldsymbol{x}^r, \boldsymbol{x}^s)}{c}) \right),$$

where L_p denotes the length of the p-th trajectory, defined in Eq. (36). Note that $\mathbb{E}[g(\boldsymbol{x}^r, \boldsymbol{x}^s, t)]$ is an even function of time. However, by definition, the RIR $h(\boldsymbol{x}^r, \boldsymbol{x}^s, t)$ is a causal function. Therefore, $\mathbb{E}[h(\boldsymbol{x}^r, \boldsymbol{x}^s, t)]$ is obtained by adding to $\mathbb{E}[g(\boldsymbol{x}^r, \boldsymbol{x}^s, t)]$ the appropriate odd solution of the homogeneous wave equation [Eq. (1)], which is such that the resulting function is causal:

$$\begin{aligned} \mathbb{E}[h(\boldsymbol{x}^r, \boldsymbol{x}^s, t)] = &\ \mathbb{E}[g(\boldsymbol{x}^r, \boldsymbol{x}^s, t)] + \frac{1}{8\pi L_p(\boldsymbol{x}^r, \boldsymbol{x}^s)} \sum_p \epsilon^{r_p} \left(\delta(t - \tfrac{L_p(\boldsymbol{x}^r, \boldsymbol{x}^s)}{c}) - \delta(t + \tfrac{L_p(\boldsymbol{x}^r, \boldsymbol{x}^s)}{c}) \right) \\ = &\ \sum_p \epsilon^{r_p} \frac{\delta(t - \frac{L_p(\boldsymbol{x}^r, \boldsymbol{x}^s)}{c})}{4\pi L_p(\boldsymbol{x}^r, \boldsymbol{x}^s)}. \end{aligned} \tag{57}$$

As expected, the mean of the RIR contains exactly the early reverberation predicted by geometrical acoustics, which is formed of the direct path for $p = 0$ (spherical wave propagating from to the punctual source $\boldsymbol{x}^s$ to the receiver $\boldsymbol{x}^r$, as in Eq. (4)), if this path is not blocked by an obstacle, and the first echos (spherical waves propagating from to the image sources to the receiver). Since in practice the sum over p is finite as explained in Sec. 3.2.4, the mean of the RIR is zero after a finite time.

Alternatively, if we consider the universal pseudo-correlation function in Eq. (26) along with the modal density in Eq. (13), as explained in Sec. 3.3, then the mathematical expectation of the RIR is calculated in Appendix B.1:

$$\mathbb{E}[h(\boldsymbol{x}^r, \boldsymbol{x}^s, t)] = \frac{\delta(t - \frac{\|\boldsymbol{x}^r - \boldsymbol{x}^s\|_2}{c})}{4\pi \|\boldsymbol{x}^r - \boldsymbol{x}^s\|_2} + \frac{\epsilon \lambda c S(\partial V)}{16\pi \|\boldsymbol{x}^r - \boldsymbol{x}^s\|_2} H(t) \ln \left| \frac{t + \frac{\|\boldsymbol{x}^r - \boldsymbol{x}^s\|_2}{c}}{t - \frac{\|\boldsymbol{x}^r - \boldsymbol{x}^s\|_2}{c}} \right|, \tag{58}$$

where $H(t)$ denotes the Heaviside function, which is such that $H(t) = 1 \ \forall t > 0$ and $H(t) = 0$ $\forall t < 0$.

[2] Note that two different integration contours must be considered, which both contain an interval of $\mathbb{R}$ centered at $f = 0$, one contour in the upper half complex plane, and the other in the lower half complex plane, depending on the sign of t. Moreover, the denominator in the right member of Eq. (55) contains two real poles at $f = c\kappa$ and $f = -c\kappa$, which belong to the integration contour, so the corresponding residues are divided by two.

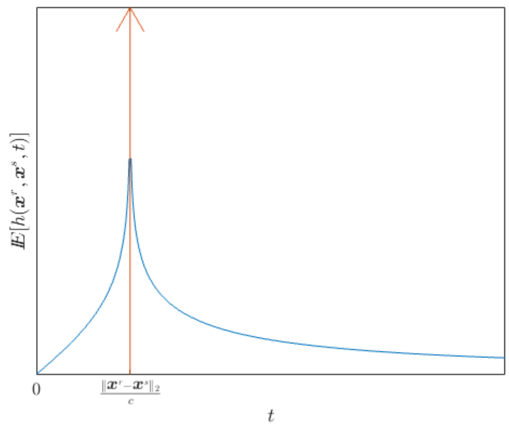

Figure 2: Representation of the mean of the RIR $\mathbb{E}[h(\boldsymbol{x}^r, \boldsymbol{x}^s, t)]$, obtained in the Neumann case with the universal pseudo-correlation function. The red arrow represents the direct path, and the blue curve represents an average of the first order reflections.

The mean of the RIR $\mathbb{E}[h(\boldsymbol{x}^r, \boldsymbol{x}^s, t)]$ expressed in Eq. (58) is illustrated in Fig. 2, in the Neumann case ($\epsilon = 1$). In the right member of Eq. (58):

- the first term, represented by the red arrow in Fig. 2, is the free field impulse response introduced in Eq. (4), which corresponds to the direct path, as in Eq. (57) for $p = 0$ if this path is not blocked by an obstacle; it is zero after a finite time;
- the second term, represented by the blue curve in Fig. 2, is a universal surface term, independent of the room's geometry, which is an average of the first order reflections. Clearly, the universal pseudo-correlation function, along with the modal density in Eq. (13), is not able to account for the fact that the first reflections necessarily arrive *after* the direct path. In other respects, this second term is asymptotically equivalent to $\frac{\lambda S(\partial V)}{8\pi t}$ when $t \to +\infty$. Therefore, its time-frequency distribution is negligible, asymptotically over time, at non-zero frequencies.[3]

We conclude that the time-frequency distribution of $\mathbb{E}[h(\boldsymbol{x}^r, \boldsymbol{x}^s, t)]$ is asymptotically negligi-

[3]Indeed, for a given $\tau > 0$, let us define the time-frequency atom $\psi_{f_0,t_0}(t) = \frac{t}{t_0} e^{-\pi \frac{(t-t_0)^2}{\tau^2} + \imath 2\pi f_0 t}$, whose Fourier transform is

$$\widehat{\psi}_{f_0,t_0}(f) = \tau \left(1 - \imath \tau^2 \frac{f - f_0}{t_0}\right) e^{-\pi \tau^2 (f-f_0)^2 - \imath 2\pi (f - f_0) t_0}.$$

Let us then consider the asymptotics $t_0 \gg \tau$, and note that $\psi_{f_0,t_0}(t)$ is not negligible only when $|t - t_0| \ll \tau$, and $\widehat{\psi}_{f_0,t_0}(f)$ is not negligible only when $|f - f_0| \ll \frac{1}{\tau}$. We then get asymptotically $|\psi_{f_0,t_0}(t)| \sim e^{-\pi \frac{(t-t_0)^2}{\tau^2}}$ and $|\widehat{\psi}_{f_0,t_0}(f)| \sim \tau e^{-\pi\tau^2(f-f_0)^2}$, so this atom is asymptotically equivalent to a Gabor atom centered at (f_0, t_0) and scaled by τ. However, the dot product of function $t \mapsto \frac{1}{t}$ with $\psi_{f_0,t_0}(t)$ is such that $\left|\int \frac{1}{t}\, \overline{\psi_{f_0,t_0}(t)} dt\right| = \tau \frac{e^{-\pi\tau^2 f_0^2}}{t_0}$. Since this equality holds for arbitrarily large values of τ, we conclude that the time-frequency distribution of function $t \mapsto \frac{1}{t}$ is asymptotically equivalent to $\frac{\delta(f_0)}{t_0}$ when $t_0 \to +\infty$.

ble when $f, t \to +\infty$, independently of the chosen pseudo-correlation function.

4.3.2. Second order moments

For all $K \in \mathbb{R}$, let $\kappa(K)$ be the unique complex solution to the equation $\mathcal{K}(K, \kappa(K)) = \kappa(K)$ with both nonnegative real and imaginary parts, whose first order asymptotic expansion was calculated in Badeau (2024, Eq. (117)):

$$\begin{aligned}\kappa(K) = \;& K + \frac{\imath\lambda}{8\pi}\int_{\boldsymbol{s}\in\partial V}\Bigg(\ln\left(\frac{1+\widehat{\beta}(\boldsymbol{s},K)}{1-\widehat{\beta}(\boldsymbol{s},K)}\right) \\ & -\widehat{\beta}(\boldsymbol{s},K)^2\ln\left(\frac{\widehat{\beta}(\boldsymbol{s},K)+1}{\widehat{\beta}(\boldsymbol{s},K)-1}\right) + 2\widehat{\beta}(\boldsymbol{s},K)\Bigg)dS(\boldsymbol{s}).\end{aligned} \tag{59}$$

Then, the following first order expansion of the second order moments of the RIR is established in Appendix B.2:

$$\begin{aligned}&\mathbb{E}[h(\boldsymbol{x}_1^r, \boldsymbol{x}_1^s, t_1)\, h(\boldsymbol{x}_2^r, \boldsymbol{x}_2^s, t_2)] \\ =\;& \frac{c^2}{8\pi^2}H(t_1)H(t_2)\,\mathrm{Re}\int_{k\in\mathbb{R}_+} \\ & \Big(\gamma(\boldsymbol{x}_1^r, \boldsymbol{x}_2^r, \mathring{\kappa}(k))\,\gamma(\boldsymbol{x}_1^s, \boldsymbol{x}_2^s, \mathring{\kappa}(k)) \\ & +\gamma(\boldsymbol{x}_1^r, \boldsymbol{x}_2^s, \mathring{\kappa}(k))\,\gamma(\boldsymbol{x}_1^s, \boldsymbol{x}_2^r, \mathring{\kappa}(k)) \\ & -C(\boldsymbol{x}_1^r, \boldsymbol{x}_1^s, \mathring{\kappa}(k))\,C(\boldsymbol{x}_2^r, \boldsymbol{x}_2^s, \overline{\mathring{\kappa}(k)})\,b\left(\frac{t_1+t_2}{2t_\kappa(k)}\right)\Big) \\ & \times\frac{e^{-4\pi c\mathrm{Im}(\mathring{\kappa}(k))\frac{t_1+t_2}{2}+\imath 2\pi ck(t_1-t_2)}}{|\mathring{\kappa}(k)|^2}\widehat{\Gamma}_\kappa(k)dk,\end{aligned} \tag{60}$$

where the form factor $b(.)$ was defined in Eq. (21), and with the following notation:

$$\mathring{\kappa}(k) = k + \imath\mathrm{Im}\kappa\left((\mathrm{Re}\kappa)^{-1}(k)\right), \tag{61}$$

$$t_\kappa(k) = t_H\left((\mathrm{Re}\kappa)^{-1}(k), 0\right), \tag{62}$$

where $t_H(K, 0) = \frac{\rho(K,0)}{c}$ is the Heisenberg time that was defined in Eq. (31), and

$$\widehat{\Gamma}_\kappa(k) = \frac{\widehat{\Gamma}_B\left((\mathrm{Re}\kappa)^{-1}(k)\right)}{(\mathrm{Re}\kappa)'((\mathrm{Re}\kappa)^{-1}(k))}, \tag{63}$$

where

$$\widehat{\Gamma}_B(K) = \lambda^2\rho(K, 0) \tag{64}$$

is the power spectral density that was originally introduced in Badeau (2024, Eq. (71)).

Note that, if we assume that $\frac{d\widehat{\beta}(\boldsymbol{s},k)}{dk} = O(\frac{1}{k})$, then substituting Eq. (59) into Eq. (61) yields the following first order asymptotic expansion:

$$\mathring{\kappa}(k) = k + \imath\mathrm{Im}\kappa(k). \tag{65}$$

In Eq. (60), in order to simplify the notations, we have introduced

$$C(\boldsymbol{x}_1, \boldsymbol{x}_2, \kappa) \triangleq C(\boldsymbol{x}_1, \boldsymbol{x}_2, \kappa, \kappa), \tag{66}$$

and

$$\gamma(\boldsymbol{x}_1, \boldsymbol{x}_2, \kappa(K)) \triangleq \gamma(\boldsymbol{x}_1, \boldsymbol{x}_2, K, \kappa(K), \kappa(K)). \tag{67}$$

Note that, in Badeau (2026d, Remarks 1 and 2), we showed that function $\gamma(\boldsymbol{x}_1, \boldsymbol{x}_2, K, k, k)$, as expressed in either Eq. (28) or Eq. (38), depends on K only through $\mathcal{K}(K, k)$. Consequently, for $k = \kappa(K)$, since $\mathcal{K}(K, \kappa(K)) = \kappa(K)$, the right member of Eq. (67) actually depends only on $\kappa(K)$. This explains why in Eq. (67), the parameter K has been omitted from the list of arguments of the γ function defined in the left member.

Finally, the possible choices of the (pseudo)-correlation functions yield different expressions of functions C, γ, t_κ, and $\widehat{\Gamma}_\kappa$, as shown below.

Universal (pseudo-)correlation functions. First, if we consider the universal (pseudo-)correlation functions described in Sec. 3.2.2 along with the modal density in Eq. (13), as explained in Sec. 3.3, then Eqs. (66) and (26) yield

$$C(\boldsymbol{x}_1, \boldsymbol{x}_2, \kappa) = \operatorname{sinc}\left(2\pi\kappa\|\boldsymbol{x}_1 - \boldsymbol{x}_2\|_2\right),$$

and Eqs. (67) and (28) yield

$$\gamma(\boldsymbol{x}_1, \boldsymbol{x}_2, \kappa(K)) = \frac{1}{4\pi}\int_{\boldsymbol{u}\in\mathcal{S}(0,1)} e^{\imath 2\pi \boldsymbol{u}^\top\left(\kappa(K)\,\boldsymbol{x}_1 - \overline{\kappa(K)}\,\boldsymbol{x}_2\right) - 2\,\mathrm{Im}(\theta(\boldsymbol{u},K,\kappa(K)))} dS(\boldsymbol{u}).$$

If we assume that $\frac{d\widehat{\beta}(\boldsymbol{s},k)}{dk} = O(\frac{1}{k})$, then substituting Eqs. (31) and (59) into Eq. (62) yields

$$\begin{aligned} t_\kappa(k) = \ & \frac{4\pi|V|}{c}\bigg(k^2 + \frac{\lambda k S(\partial V)}{8} + \frac{\lambda k}{4\pi}\mathrm{Im}\int_{\boldsymbol{s}\in\partial V}\bigg(\ln\left(\frac{1+\widehat{\beta}(\boldsymbol{s},k)}{1-\widehat{\beta}(\boldsymbol{s},k)}\right) \\ & -\widehat{\beta}(\boldsymbol{s},k)^2\ln\left(\frac{\widehat{\beta}(\boldsymbol{s},k)+1}{\widehat{\beta}(\boldsymbol{s},k)-1}\right) + 2\widehat{\beta}(\boldsymbol{s},k)\bigg)dS(\boldsymbol{s})\bigg). \end{aligned}$$

If in addition, we assume that $\frac{d\widehat{\beta}(\boldsymbol{s},k)}{dk} = o(\frac{1}{k})$, then substituting Eq. (59) into Eq. (63) yields

$$\begin{aligned} \widehat{\Gamma}_\kappa(k) = \ & 4\pi\lambda\bigg(k^2 + \frac{\lambda k S(\partial V)}{8} + \frac{\lambda k}{4\pi}\mathrm{Im}\int_{\boldsymbol{s}\in\partial V}\bigg(\ln\left(\frac{1+\widehat{\beta}(\boldsymbol{s},k)}{1-\widehat{\beta}(\boldsymbol{s},k)}\right) \\ & -\widehat{\beta}(\boldsymbol{s},k)^2\ln\left(\frac{\widehat{\beta}(\boldsymbol{s},k)+1}{\widehat{\beta}(\boldsymbol{s},k)-1}\right) + 2\widehat{\beta}(\boldsymbol{s},k)\bigg)dS(\boldsymbol{s})\bigg). \end{aligned}$$

Multiple-path (pseudo-)correlation functions. If we consider the multiple-path (pseudo-)correlation functions described in Sec. 3.2.4 along with the modal density in Eq. (12), as explained in Sec. 3.3, then Eqs. (66) and (37) yield

$$\begin{aligned} C(\boldsymbol{x}_1, \boldsymbol{x}_2, \kappa) = \ & \sum_p \frac{1}{4\pi}\int_{\boldsymbol{u}\in\mathcal{S}(0,1)}\left(\prod_{q=0}^{r_p-1}\frac{\boldsymbol{u}^\top\boldsymbol{R}_{p,r_p-1}\ldots\boldsymbol{R}_{p,q+1}\boldsymbol{n}(\boldsymbol{s}_{p,q}) - \widehat{\beta}(\boldsymbol{s}_{p,q},\kappa)}{\boldsymbol{u}^\top\boldsymbol{R}_{p,r_p-1}\ldots\boldsymbol{R}_{p,q+1}\boldsymbol{n}(\boldsymbol{s}_{p,q}) + \widehat{\beta}(\boldsymbol{s}_{p,q},\kappa)}\right) \\ & \times\frac{e^{\imath 2\pi\kappa\boldsymbol{u}^\top(\boldsymbol{x}_1 - \boldsymbol{Q}_p\boldsymbol{x}_2 - \boldsymbol{y}_p)} + e^{\imath 2\pi\kappa\boldsymbol{u}^\top(\boldsymbol{x}_2 - \boldsymbol{Q}_p\boldsymbol{x}_1 - \boldsymbol{y}_p)}}{2}dS(\boldsymbol{u}), \end{aligned}$$

and Eqs. (67), (38) and (39) yield

$$\gamma(\boldsymbol{x}_1, \boldsymbol{x}_2, \kappa(K)) = \frac{\mathring{\gamma}(\boldsymbol{x}_1,\boldsymbol{x}_2,\kappa(K)) + \overline{\mathring{\gamma}(\boldsymbol{x}_2,\boldsymbol{x}_1,\kappa(K)}}{2},$$

with

$$\mathring{\gamma}(\boldsymbol{x}_1, \boldsymbol{x}_2, \kappa(K)) = \sum_p \frac{1}{4\pi} \int_{\boldsymbol{u}\in\mathcal{S}(0,1)} e^{\imath 2\pi \boldsymbol{u}^\top \left(\kappa(K)\boldsymbol{x}_1 - \overline{\kappa(K)}\boldsymbol{Q}_p \boldsymbol{x}_2 - K\boldsymbol{y}_p\right)} \times e^{\imath\left(\theta(\boldsymbol{u},K,\kappa(K)) - \overline{\theta\left(\boldsymbol{Q}_p^\top \boldsymbol{u},K,\kappa(K)\right)}\right)} dS(\boldsymbol{u}).$$

If we assume that $\frac{d\widehat{\beta}(\boldsymbol{s},k)}{dk} = O(\frac{1}{k})$, then substituting Eqs. (31) and (59) into Eq. (62) yields

$$t_\kappa(k) = \frac{4\pi|V|}{c}\Bigg(k^2 + \frac{\lambda k}{4\pi}\mathrm{Im}\int_{\boldsymbol{s}\in\partial V}\Bigg(\ln\left(\frac{1+\widehat{\beta}(\boldsymbol{s},k)}{1-\widehat{\beta}(\boldsymbol{s},k)}\right) - \widehat{\beta}(\boldsymbol{s},k)^2 \ln\left(\frac{\widehat{\beta}(\boldsymbol{s},k)+1}{\widehat{\beta}(\boldsymbol{s},k)-1}\right) + 2\widehat{\beta}(\boldsymbol{s},k)\Bigg)dS(\boldsymbol{s})\Bigg).$$

If in addition, we assume that $\frac{d\widehat{\beta}(\boldsymbol{s},k)}{dk} = o(\frac{1}{k})$, then substituting Eq. (59) into Eq. (63) yields

$$\widehat{\Gamma}_\kappa(k) = 4\pi\lambda\Bigg(k^2 + \frac{\lambda k}{4\pi}\mathrm{Im}\int_{\boldsymbol{s}\in\partial V}\Bigg(\ln\left(\frac{1+\widehat{\beta}(\boldsymbol{s},k)}{1-\widehat{\beta}(\boldsymbol{s},k)}\right) - \widehat{\beta}(\boldsymbol{s},k)^2 \ln\left(\frac{\widehat{\beta}(\boldsymbol{s},k)+1}{\widehat{\beta}(\boldsymbol{s},k)-1}\right) + 2\widehat{\beta}(\boldsymbol{s},k)\Bigg)dS(\boldsymbol{s})\Bigg).$$

4.3.3. Wigner distribution

The definition of the cross-Wigner distribution of the RIR in Eq. (41) involves the ACF Γ_h defined in Eq. (40). However, we have shown in Sec. 4.3.1, in the case of Neumann and Dirichlet boundary conditions, that the time-frequency distribution of $\mathbb{E}[h(\boldsymbol{x}^r, \boldsymbol{x}^s, t)]$ is asymptotically negligible when $f, t \to +\infty$. In fact, this remark also holds in the general case of the complex Robin boundary condition, because $\mathbb{E}[h(\boldsymbol{x}^r, \boldsymbol{x}^s, t)]$ still contains only the direct path and the first echoes. Therefore the ACF $\Gamma_h(\boldsymbol{x}_1^r, \boldsymbol{x}_1^s, \boldsymbol{x}_2^r, \boldsymbol{x}_2^s, t_1, t_2)$ can be asymptotically identified to the second order moments $\mathbb{E}[h(\boldsymbol{x}_1^r, \boldsymbol{x}_1^s, t_1)\, h(\boldsymbol{x}_2^r, \boldsymbol{x}_2^s, t_2)]$ calculated in Eq. (60).

In other respects, because the RIR is a causal function of time, calculating the exact Wigner distribution of the RIR from Eq. (60) would produce spurious interference terms that are a well-known, undesirable property of the Wigner distribution (Cohen, 1989). Instead, in order to cancel out these interference terms, we consider the natural continuation of the RIR to negative times, which is actually an *odd* function of time. This change just amounts to removing the terms $H(t_1)$ and $H(t_2)$ from Eq. (60).

Finally, Eq. (60) modified in this way, with the change of variable $k = \frac{f}{c}$, shows that the cross-Wigner distribution of the RIR defined in Eq. (41) is expressed as

$$W_h(\boldsymbol{x}_1^r, \boldsymbol{x}_1^s, \boldsymbol{x}_2^r, \boldsymbol{x}_2^s, f, t) = \frac{c^3\widehat{\Gamma}_\kappa(\frac{f}{c})}{4}\Bigg(\frac{\gamma(\boldsymbol{x}_1^r,\boldsymbol{x}_2^r,\mathring{\kappa}(\frac{f}{c}))\,\gamma(\boldsymbol{x}_1^s,\boldsymbol{x}_2^s,\mathring{\kappa}(\frac{f}{c})) + \gamma(\boldsymbol{x}_1^r,\boldsymbol{x}_2^s,\mathring{\kappa}(\frac{f}{c}))\,\gamma(\boldsymbol{x}_1^s,\boldsymbol{x}_2^r,\mathring{\kappa}(\frac{f}{c}))}{4\pi^2 f^2 + \alpha(\frac{f}{c})^2} - \frac{C(\boldsymbol{x}_1^r,\boldsymbol{x}_1^s,\mathring{\kappa}(\frac{f}{c}))\,\overline{C(\boldsymbol{x}_2^r,\boldsymbol{x}_2^s,\mathring{\kappa}(\frac{f}{c}))}\, b\left(\frac{t}{t_\kappa(f/c)}\right)}{4\pi^2 f^2 + \alpha(\frac{f}{c})^2}\Bigg) e^{-2\alpha(\frac{f}{c})t}, \tag{68}$$

where functions t_κ, $\widehat{\Gamma}_\kappa$, $\mathring{\kappa}$, C and γ were defined in Eqs. (62), (63), (65), (66) and (67), respectively, and $\alpha(k) \triangleq 2\pi c \mathrm{Im}(\mathring{\kappa}(k))$ is the *temporal attenuation*. These various functions can further be expressed according to the selected (pseudo-)correlation functions, as shown in Secs. 4.3.2 and 4.3.2. It can be noted that Eq. (68) satisfies the acoustic reciprocity principle: it remains unchanged when the positions of the source and the receiver are swapped, i.e., whether $\boldsymbol{x}_1^s$ is swapped with $\boldsymbol{x}_1^r$, or $\boldsymbol{x}_2^s$ is swapped with $\boldsymbol{x}_2^r$. In addition, Eq. (68) can be simplified by noting that when $f \to +\infty$,

$$\frac{c^3\widehat{\Gamma}_\kappa(\frac{f}{c})}{4(4\pi^2 f^2+\alpha(\frac{f}{c})^2)} \longrightarrow \frac{\lambda c}{4\pi}.$$

Finally, the expression of the power distribution is obtained by taking $\boldsymbol{x}_1^r = \boldsymbol{x}_2^r = \boldsymbol{x}^r$ and $\boldsymbol{x}_1^s = \boldsymbol{x}_2^s = \boldsymbol{x}^s$ in Eq. (68):

$$\begin{aligned} W_h(\boldsymbol{x}^r, \boldsymbol{x}^s, f, t) \triangleq\ & W_h(\boldsymbol{x}^r, \boldsymbol{x}^s, \boldsymbol{x}^r, \boldsymbol{x}^s, f, t) \\ =\ & \frac{c^3\widehat{\Gamma}_\kappa(\frac{f}{c})}{4}\Bigg(\frac{\gamma(\boldsymbol{x}^r,\boldsymbol{x}^r,\mathring{\kappa}(\frac{f}{c}))\,\gamma(\boldsymbol{x}^s,\boldsymbol{x}^s,\mathring{\kappa}(\frac{f}{c}))+\big|\gamma(\boldsymbol{x}^r,\boldsymbol{x}^s,\mathring{\kappa}(\frac{f}{c}))\big|^2}{4\pi^2 f^2+\alpha(\frac{f}{c})^2} \\ & -\frac{\big|C(\boldsymbol{x}^r,\boldsymbol{x}^s,\mathring{\kappa}(\frac{f}{c}))\big|^2\, b\Big(\frac{t}{t_\kappa(f/c)}\Big)}{4\pi^2 f^2+\alpha(\frac{f}{c})^2}\Bigg)e^{-2\alpha(\frac{f}{c})t}. \end{aligned} \tag{69}$$

In the Neumann case, Eq. (68) is simplified as follows:

$$\begin{aligned} W_h(\boldsymbol{x}_1^r, \boldsymbol{x}_1^s, \boldsymbol{x}_2^r, \boldsymbol{x}_2^s, f, t) =\ & \frac{c^3\widehat{\Gamma}_B(\frac{f}{c})}{4}\Bigg(\frac{C(\boldsymbol{x}_1^r,\boldsymbol{x}_2^r,\frac{f}{c})\,C(\boldsymbol{x}_1^s,\boldsymbol{x}_2^s,\frac{f}{c})+C(\boldsymbol{x}_1^r,\boldsymbol{x}_2^s,\frac{f}{c})\,C(\boldsymbol{x}_1^s,\boldsymbol{x}_2^r,\frac{f}{c})}{4\pi^2 f^2} \\ & -\frac{C(\boldsymbol{x}_1^r,\boldsymbol{x}_1^s,\frac{f}{c})\,C(\boldsymbol{x}_2^r,\boldsymbol{x}_2^s,\frac{f}{c})\,b\Big(\frac{t}{t_H(f/c,0)}\Big)}{4\pi^2 f^2}\Bigg), \end{aligned} \tag{70}$$

where t_H is the Heisenberg time defined in Eq. (31), and $\widehat{\Gamma}_B$ is the power spectral density defined in Eq. (64). In the same way, Eq. (69) becomes

$$W_h(\boldsymbol{x}^r, \boldsymbol{x}^s, f, t) = \frac{c^3\widehat{\Gamma}_B(\frac{f}{c})}{4}\Bigg(\frac{C(\boldsymbol{x}^r,\boldsymbol{x}^r,\frac{f}{c})\,C(\boldsymbol{x}^s,\boldsymbol{x}^s,\frac{f}{c})}{4\pi^2 f^2} + \frac{\Big(C(\boldsymbol{x}^r,\boldsymbol{x}^s,\frac{f}{c})\Big)^2\Big(1-b\Big(\frac{t}{t_H(f/c,0)}\Big)\Big)}{4\pi^2 f^2}\Bigg). \tag{71}$$

Eq. (71) shows that, at fixed source position $\boldsymbol{x}^s$, the power of the wave field is enhanced in the vicinity of $\boldsymbol{x}^s$: we retrieve the enhanced backscattering phenomenon discussed in Sec. 3.2.3.

Finally, let us consider the universal pseudo-correlation function in Eq. (26) along with the modal density in Eq. (13), as explained in Sec. 3.3. Then, Eq. (71) is simplified as follows:

$$W_h(\boldsymbol{x}^r, \boldsymbol{x}^s, f, t) = \frac{c^3\widehat{\Gamma}_B(\frac{f}{c})}{4}\,\frac{1+\Big(C(\boldsymbol{x}^r,\boldsymbol{x}^s,\frac{f}{c})\Big)^2\Big(1-b\Big(\frac{t}{t_H(f/c,0)}\Big)\Big)}{4\pi^2 f^2}. \tag{72}$$

In addition, when $\boldsymbol{x}_1^s = \boldsymbol{x}_2^s = \boldsymbol{x}^s$, far from the source $\boldsymbol{x}^s$, Eq. (70) further simplifies as:

$$W_h(\boldsymbol{x}_1^r, \boldsymbol{x}^s, \boldsymbol{x}_2^r, \boldsymbol{x}^s, f, t) = \frac{c^3\widehat{\Gamma}_B(\frac{f}{c})}{4}\,\frac{\operatorname{sinc}(2\pi\frac{f}{c}\|\boldsymbol{x}_1^r-\boldsymbol{x}_2^r\|_2)}{4\pi^2 f^2}. \tag{73}$$

We thus retrieve the original formula that was expressed in Badeau (2024, Eq. (89)). Note that this expression is a function of $\|\boldsymbol{x}_1^r - \boldsymbol{x}_2^r\|_2$, and it is independent of the source position $\boldsymbol{x}^s$. We retrieve the fact that the wave field behaves like a centered and isotropic stationary random process, provided that $t \to +\infty$ and $f \to +\infty$.

5. Discussion and conclusion

In this paper, the mathematical foundations of the statistical wave field theory have been reworked at the fundamental level of the eigenspectrum and eigenfunctions of the complex Robin Laplacian. We first identified the relevant works regarding the asymptotic distribution of the *eigenspectrum* of the *real* Robin Laplacian (Sec. 3.1), which include the asymptotic expansion of the modal density (Weyl's law for the volume term and Balian and Bloch (1970) formula for the first order surface term), the identification of the wave number distortion (Badeau, 2024), and the probability distribution of the eigenspectrum predicted by the random matrix theory (Mehta, 1991). Then we identified the relevant works regarding the asymptotic distribution of the *eigenfunctions* of the *real* Robin Laplacian, which include the Gaussian RWM and universal correlation function (Berry, 1977), the enhanced backscattering phenomenon (Weaver and Lobkis, 2000), and the multiple-path correlation function (Hortikar and Srednicki, 1998) (Sec. 3.2).

Based on these existing works, we introduced in Badeau (2026d, Sec. IV) a general RWM of the eigenfunctions of the complex Robin Laplacian, which is also summarized in Sec. 3.2. This contribution was twofold: first, it unifies the existing RWMs dedicated to the real Robin Laplacian, and second, it generalizes these RWMs to the *complex* Robin Laplacian, which makes it possible to account for the absorption of energy at the boundary surface. Next, in this paper, we paid particular attention to ensuring consistency between the eigenspectrum model and the RWM of the eigenfunctions (Sec. 3.3). Indeed, two combinations are possible. When the room's geometry is unknown, the universal correlation function, which ignores the reflections at the boundary, can be complemented by the asymptotic expansion of the modal density that includes the first order surface term (Balian and Bloch, 1970), which accounts for first order reflections. Alternatively, when the exact room's geometry is known, the multiple-path correlation function, which innately takes the first reflections at the boundary into account, can be complemented by the asymptotic expansion of the modal density that includes only the volume term, without the first order surface term (Weyl's law).

Then, based on these probabilistic models of the eigenspectrum and eigenfunctions of the complex Robin Laplacian, we were able to calculate the first and second order statistics of the wave field (Sec. 4). We thus achieved an expected and remarkable result: the unification of geometrical acoustics (Kuttruff, 2014, Chap. 4), which is generally used to predict the first echoes that appear in early reverberation, and of probabilistic models (Kuttruff, 2014, Chap. 5), which are generally used to predict the statistical properties of late reverberation. More precisely, the predictions of early reverberation (direct path and first echos) from geometrical acoustics are retrieved in the first order statistics of the RIR (Sec. 4.3.1). With the multiple-path pseudo-correlation function, the first echos are represented accurately given the exact room's geometry, whereas they are averaged over time and space, independently of the room's geometry, with the universal pseudo-correlation function. Moreover, the predictions of late reverberation (power distribution over space, frequency and time) are retrieved in the second order statistics of the RIR (Sec. 4.3.2), as in our previous works on the statistical wave field theory.

Incidentally, we obtained several other known results. First, the former third assumption of the statistical wave field theory, which states that the mean and pseudo-covariances of the B-function are stationary (Badeau, 2024), is now a mathematical result proved from the RWM introduced in Badeau (2026d, Sec. IV) (Appendix A.2). Consequently, we also retrieved the former predictions of the statistical wave field theory (Sec. 4.3.2). In the case of Neumann's boundary condition, we thus retrieved the formula of the power distribution over time, frequency, and space, which is proportional to the modal density, based on the universal correlation function and on the asymptotic expansion of the modal density up to the first order surface term (Balian and Bloch, 1970). In the case of Robin's boundary condition, the closed-form expressions of the wave number distortion and of the reverberation time are the same as in our previous works. In addition, the enhanced backscattering phenomenon (Weaver and Lobkis, 2000) is now accounted for, based on existing results from random matrix theory (Sec. 4.3.2).

In addition to the previously mentioned contributions, various other improvements have been made compared to the existing works. First, we have proved the almost sure convergence of the series that defines the B-function of the complex Robin Laplacian in the case of mixing billiards (Appendix A.1). This is a simplification of the general result that we had previously obtained in Badeau (2025a), by following a completely different approach. Other improvements include the accurate prediction of the first echos in the case of energy absorption (Sec. 4.3.1), compared to the usual approximation by punctual image sources in geometrical acoustics (Kuttruff, 2014, Chap. 4), and the accurate prediction of the power distribution over time, frequency and space compared to our previous works, which was the initial impetus for the research presented in this article, and which now respects the acoustic reciprocity principle (Sec. 4.3.3). Finally, another contribution is the generalization of the enhanced backscattering formulas (Weaver and Lobkis, 2000) to the complex Robin Laplacian, which takes energy absorption into account (Sec. 4.3.3).

The possible future extensions and applications of the work presented in this article are numerous. For instance, the curvature of the boundary surface was taken into account to improve the predictions of the wave number distortion and of the reverberation time in Badeau (2025b), based on the second order curvature term in the asymptotic expansion of the modal density (Balian and Bloch, 1970). From the new perspective adopted in this article, we know that this second order asymptotic expansion can be combined with the universal (pseudo-)correlation functions, to get a space-averaged improved prediction of the power distribution, independent of the room's geometrical shape. Alternatively, the curvature of the boundary could also be taken into account in the multiple-path (pseudo-)correlation functions, which can be combined with Weyl's law, in order to get an even more accurate prediction of the power distribution, when the exact room's geometry is known.

Acknowledgments

The author would like to thank Gregor Tanner for interesting discussions, and for drawing his attention to the existing works on enhanced backscattering (Weaver and Lobkis, 2000) and on the multiple-path correlation function (Hortikar and Srednicki, 1998), which are mentioned in his topical review paper (Tanner and Søndergaard, 2007).

Author Declarations

Conflict of Interest: The author of this paper has no conflict of interest to disclose.

Data Availability

Data sharing is not applicable to this article as no new data were created or analyzed in this study.

Appendix A. Properties of the B-function

In this appendix, we study the convergence of the series that defines the B-function (Appendix A.1), and prove the former third assumption of the statistical wave field theory (Appendix A.2).

Appendix A.1. Convergence of the B-function to a distribution

In the case of the real Robin Laplace operator, it is well known that the series that defines the B-function in Eq. (42) deterministically converges in V to the identity operator on the Hilbert space of square integrable functions $L^2(V)$. However, in the general case of the complex Robin Laplace operator, there is no guarantee of convergence of this series. Instead, we were able to prove in Badeau (2025a) the convergence in a weaker sense, which is related to the notion of *Abel basis with brackets* mentioned in Sec. 2.4: $B(\boldsymbol{y}^r, \boldsymbol{x}^s, k) = \lim_{\varepsilon\to 0^+} B(\boldsymbol{y}^r, \boldsymbol{x}^s, k, \varepsilon)$, with

$$B(\boldsymbol{y}^r, \boldsymbol{x}^s, k, \varepsilon) \triangleq \sum_{m\in\mathbb{N}} \left[\sum_{n=N_m}^{N_{m+1}-1} e^{-\varepsilon\,\lambda_n(k)^\gamma} \varphi_n(\boldsymbol{y}^r, k)\varphi_n(\boldsymbol{x}^s, k)\right], \tag{A.1}$$

where $\{\lambda_n(k)\}_{n\in\mathbb{N}}$ are the eigenvalues of the Robin Laplace operator, $\gamma \geq 0$ is the order of the Abel basis, and $\{N_m\}_{m\in\mathbb{N}}$ is an increasing sequence of natural numbers, such that $N_0 = 0$. In Eq. (A.1), the convergence of the series is guaranteed thanks to the exponential weights $e^{-\varepsilon\,\lambda_n(k)^\gamma}$, and then the sum of the series converges as a function of ε when $\varepsilon \to 0$. Due to the presence of the brackets in Eq. (A.1), the convergence of the series is *conditional* (i.e., the terms of this series must be sorted in this particular order).

In this section, we will be able to prove that if the eigenfunctions follow the general RWM introduced in Badeau (2026d, Sec. IV), then there is no longer any need to refer to the difficult concept of Abel basis with brackets: the usual series in Eq. (42) converges to a distribution on $\mathbb{R}^3$ *almost surely*, i.e., for almost every mixing billiard. However, remember that the eigenfunction statistics implicitly involve averages over a small bandwidth as explained at the beginning of Sec. 3.2. So, we actually retrieve there a notion that is similar to that of the series "with brackets" in Eq. (A.1). Therefore the convergence of the series in Eq. (42) is guaranteed almost surely, but also in the conditional sense.

More precisely, we will prove that $\forall \boldsymbol{x}^s \in V$, the series in Eq. (42) almost surely converges to a distribution defined on the set $\mathcal{D}(\mathbb{R}^3)$ of smooth functions ψ with compact support in $\mathbb{R}^3$.

Indeed, from Eq. (47), we get:

$$
\begin{aligned}
& \mathbb{E}\left[\left|\int_{\boldsymbol{y}^r\in\mathbb{R}^3}\psi(\boldsymbol{y}^r)B(\boldsymbol{y}^r,\boldsymbol{x}^s,k)d\boldsymbol{y}^r\right|^2\right] \\
= \;& \lambda^2\int_{K\in\mathbb{R}_+}\rho(K,0)\Big(\gamma(\boldsymbol{x}^s,\boldsymbol{x}^s,K,k,k) \\
& \int_{\boldsymbol{y}_1^r\in\mathbb{R}^3}\int_{\boldsymbol{y}_2^r\in\mathbb{R}^3}\psi(\boldsymbol{y}_1^r)\gamma(\boldsymbol{y}_1^r,\boldsymbol{y}_2^r,K,k,k)\overline{\psi(\boldsymbol{y}_2^r)}d\boldsymbol{y}_1^r d\boldsymbol{y}_2^r \\
& +\left|\int_{\boldsymbol{y}^r\in\mathbb{R}^3}\psi(\boldsymbol{y}^r)\gamma(\boldsymbol{y}^r,\boldsymbol{x}^s,K,k,k)d\boldsymbol{y}^r\right|^2\Big)dK \\
& +\lambda^2\iint_{K_1,K_2\in\mathbb{R}_+}\rho\left(K_1,0\right)\rho\left(K_2,0\right) \\
& \times\int_{\boldsymbol{y}_1^r\in\mathbb{R}^3}\psi(\boldsymbol{y}_1^r)\,C(\boldsymbol{y}_1^r,\boldsymbol{x}^s,\mathcal{K}(K_1,k),k)d\boldsymbol{y}_1^r \\
& \times\int_{\boldsymbol{y}_2^r\in\mathbb{R}^3}\overline{\psi(\boldsymbol{y}_2^r)\,C(\boldsymbol{y}_2^r,\boldsymbol{x}^s,\mathcal{K}(K_2,k),k)}d\boldsymbol{y}_2^r \\
& \times R_2\left((K_1-K_2)\rho\left(\tfrac{K_1+K_2}{2},0\right)\right)dK_1dK_2.
\end{aligned}
$$

However, Eq. (20) shows that $R_2=1-Y$, where function Y is bounded, as proved at the end of Sec. 3.1.3. Therefore, function R_2 is also bounded, by its supremum $\|R_2\|_\infty<+\infty$. We then get the upper bound:

$$
\begin{aligned}
& \mathbb{E}\left[\left|\int_{\boldsymbol{y}^r\in\mathbb{R}^3}\psi(\boldsymbol{y}^r)B(\boldsymbol{y}^r,\boldsymbol{x}^s,k)d\boldsymbol{y}^r\right|^2\right] \\
\leq \;& \lambda^2\int_{K\in\mathbb{R}_+}\rho(K,0)\Big(\gamma(\boldsymbol{x}^s,\boldsymbol{x}^s,K,k,k) \\
& \int_{\boldsymbol{y}_1^r\in\mathbb{R}^3}\int_{\boldsymbol{y}_2^r\in\mathbb{R}^3}\psi(\boldsymbol{y}_1^r)\gamma(\boldsymbol{y}_1^r,\boldsymbol{y}_2^r,K,k,k)\overline{\psi(\boldsymbol{y}_2^r)}d\boldsymbol{y}_1^r d\boldsymbol{y}_2^r \\
& +\left|\int_{\boldsymbol{y}^r\in\mathbb{R}^3}\psi(\boldsymbol{y}^r)\gamma(\boldsymbol{y}^r,\boldsymbol{x}^s,K,k,k)d\boldsymbol{y}^r\right|^2\Big)dK \\
& +\lambda^2\|R_2\|_\infty\Big(\int_{K\in\mathbb{R}_+}\rho\left(K,0\right) \\
& \left|\int_{\boldsymbol{y}^r\in\mathbb{R}^3}\psi(\boldsymbol{y}^r)\,C(\boldsymbol{y}^r,\boldsymbol{x}^s,\mathcal{K}(K,k),k)d\boldsymbol{y}^r\right|dK\Big)^2.
\end{aligned}
\tag{A.2}
$$

However, we have

$$
\int_{\boldsymbol{y}^r\in\mathbb{R}^3}\psi(\boldsymbol{y}^r)\gamma(\boldsymbol{y}^r,\boldsymbol{x}^s,K,k,k)d\boldsymbol{y}^r=-\frac{\int_{\boldsymbol{y}^r\in\mathbb{R}^3}\Delta\psi(\boldsymbol{y}^r)\gamma(\boldsymbol{y}^r,\boldsymbol{x}^s,K,k,k)d\boldsymbol{y}^r}{4\pi^2\mathcal{K}(K,k)^2},
$$

where function $\gamma(\boldsymbol{y}^r,\boldsymbol{x}^s,K,k,k)$, whether it is expressed as in Eq. (28) or as in Eq. (38), is bounded independently of K and k, therefore there is a constant $M_1>0$, which only depends on the compact support of ψ, such that

$$
\left|\int_{\boldsymbol{y}^r\in\mathbb{R}^3}\psi(\boldsymbol{y}^r)\gamma(\boldsymbol{y}^r,\boldsymbol{x}^s,K,k,k)d\boldsymbol{y}^r\right|\leq M_1\frac{\sup|\Delta\psi|}{|\mathcal{K}(K,k)|^2}.
$$

In the same way, we have

$$
\int_{\boldsymbol{y}^r\in\mathbb{R}^3}\psi(\boldsymbol{y}^r)\,C(\boldsymbol{y}^r,\boldsymbol{x}^s,\mathcal{K}(K,k),k)d\boldsymbol{y}^r=-\frac{\int_{\boldsymbol{y}^r\in\mathbb{R}^3}\Delta^2\psi(\boldsymbol{y}^r)C(\boldsymbol{y}^r,\boldsymbol{x}^s,\mathcal{K}(K,k),k)d\boldsymbol{y}^r}{(4\pi^2\mathcal{K}(K,k)^2)^2},
$$

where function $C(\boldsymbol{y}^r,\boldsymbol{x}^s,\mathcal{K}(K,k),k)$, whether it is expressed as in Eq. (26) or as in Eq. (37), is bounded independently of K and k, therefore there is a constant $M_2>0$, which only depends on the compact support of ψ, such that

$$
\left|\int_{\boldsymbol{y}^r\in\mathbb{R}^3}\psi(\boldsymbol{y}^r)\,C(\boldsymbol{y}^r,\boldsymbol{x}^s,\mathcal{K}(K,k),k)d\boldsymbol{y}^r\right|\leq M_2\frac{\sup\left|\Delta^2\psi\right|}{|\mathcal{K}(K,k)|^4}.
$$

In addition, there is a constant $M_3 > 0$, which only depends on the compact support of ψ, such that

$$\int_{\boldsymbol{y}_1^r\in\mathbb{R}^3}\int_{\boldsymbol{y}_2^r\in\mathbb{R}^3}\psi(\boldsymbol{y}_1^r)\gamma(\boldsymbol{y}_1^r,\boldsymbol{y}_2^r,K,k,k)\overline{\psi(\boldsymbol{y}_2^r)}d\boldsymbol{y}_1^r d\boldsymbol{y}_2^r \leq M_3\tfrac{\sup|\Delta\psi|^2}{|\mathcal{K}(K,k)|^4}.$$

Finally, we note that $\rho(K,0)$, whether it is expressed as in Eq. (12) or as in Eq. (13), grows quadratically with K, and that $\mathcal{K}(K,k)$, as expressed in Eq. (15), grows linearly with K. We deduce that $\mathbb{E}\left[\left|\int_{\boldsymbol{y}^r\in\mathbb{R}^3}\psi(\boldsymbol{y}^r)B(\boldsymbol{y}^r,\boldsymbol{x}^s,k)d\boldsymbol{y}^r\right|^2\right]$, as expressed in Eq. (A.2), is bounded by $\max\left(\sup|\Delta\psi|,\sup|\Delta^2\psi|\right)^2$, multiplied by a constant that depends on the compact support of ψ. This finally proves that the series in Eq. (42) almost surely converges to a distribution.

Appendix A.2. Former third assumption of the statistical wave field theory

In this section, we will focus on the universal pseudo-correlation function in Eq. (26) along with the modal density in Eq. (13), as explained in Sec. 3.3. Our purpose is to show that, in this case, the probability distribution of the eigenspectrum described in Sec. 3.1.3, and the RWM of the eigenfunctions introduced in Badeau (2026d, Sec. IV), jointly induce the former third assumption of the statistical wave field theory, as expressed in (Badeau, 2024, Sec. IV D): at high frequency, the mean and (pseudo-)covariances of the B-function are stationary and isotropic. This mathematical property thus becomes a mathematical result, proved from more fundamental assumptions. Note that the following mathematical developments are actually independent of the selected pseudo-correlation function; the results will be particularized to the universal pseudo-correlation function only at the end of this section.

First, regarding the mathematical expectation of the B-function, Eq. (46) shows that, in the case of Neumann and Dirichlet boundary conditions, away from the original source position, and at high frequency, $\mathbb{E}[B(\boldsymbol{y}^r,\boldsymbol{x}^s,k)]$ is negligible. This remark also holds in the general case of the complex Robin boundary condition, because $\mathbb{E}[B(\boldsymbol{y}^r,\boldsymbol{x}^s,k)]$ still contains only terms involving the original source and the first image sources. Therefore, we conclude that the B-function behaves asymptotically like a centered random process.

Next, regarding the *pseudo-covariance function* (PCF) of the B-function, the pseudo-covariances are defined as

$$\begin{aligned}&\operatorname{cov}[B(\boldsymbol{y}_1^r,\boldsymbol{x}_1^s,k),\overline{B(\boldsymbol{y}_2^r,\boldsymbol{x}_2^s,k)}]\\ =\;&\mathbb{E}[B(\boldsymbol{y}_1^r,\boldsymbol{x}_1^s,k)\,B(\boldsymbol{y}_2^r,\boldsymbol{x}_2^s,k)]-\mathbb{E}[B(\boldsymbol{y}_1^r,\boldsymbol{x}_1^s,k)]\,\mathbb{E}[B(\boldsymbol{y}_2^r,\boldsymbol{x}_2^s,k)].\end{aligned}\tag{A.3}$$

Let us first calculate the pseudo-second-order-moments of the B-function when the wave numbers are fixed, i.e., when the measure μ in Eq. (16) is deterministic, and only the eigenfunctions φ_n are random. By substituting Eq. (42) into Eq. (A.3), applying Lemma 1, and finally substituting Eq. (25), we get

$$\mathbb{E}[B(\boldsymbol{y}_1^r,\boldsymbol{x}_1^s,k)\,B(\boldsymbol{y}_2^r,\boldsymbol{x}_2^s,k)]$$

$$
\begin{aligned}
= \quad & \lambda^2 \sum_{n\in\mathbb{N}} \Big(C(\boldsymbol{y}_1^r, \boldsymbol{y}_2^r, \mathcal{K}(K_n, k), k) C(\boldsymbol{x}_1^s, \boldsymbol{x}_2^s, \mathcal{K}(K_n, k), k) \\
& + C(\boldsymbol{y}_1^r, \boldsymbol{x}_2^s, \mathcal{K}(K_n, k), k) C(\boldsymbol{x}_1^s, \boldsymbol{y}_2^r, \mathcal{K}(K_n, k), k) \Big) \\
& + \lambda^2 \sum_{n_1\in\mathbb{N}} C(\boldsymbol{y}_1^r, \boldsymbol{x}_1^s, \mathcal{K}(K_{n_1}, k), k) \\
& \times \sum_{n_2\in\mathbb{N}} C(\boldsymbol{y}_2^r, \boldsymbol{x}_2^s, \mathcal{K}(K_{n_2}, k), k) \\
= \quad & \lambda^2 \int_{K\in\mathbb{R}_+} \Big(C(\boldsymbol{y}_1^r, \boldsymbol{y}_2^r, \mathcal{K}(K, k), k) C(\boldsymbol{x}_1^s, \boldsymbol{x}_2^s, \mathcal{K}(K, k), k) \\
& + C(\boldsymbol{y}_1^r, \boldsymbol{x}_2^s, \mathcal{K}(K, k), k) C(\boldsymbol{x}_1^s, \boldsymbol{y}_2^r, \mathcal{K}(K, k), k) \Big) \\
& d\mu(K, 0) \\
& + \lambda^2 \int_{K_1\in\mathbb{R}_+} C(\boldsymbol{y}_1^r, \boldsymbol{x}_1^s, \mathcal{K}(K_1, k), k) d\mu(K_1, 0) \\
& \times \int_{K_2\in\mathbb{R}_+} C(\boldsymbol{y}_2^r, \boldsymbol{x}_2^s, \mathcal{K}(K_2, k), k) d\mu(K_2, 0),
\end{aligned}
$$

where we have substituted Eq. (16) in the last equality. Then, by applying the mathematical expectation w.r.t. the random measure μ, we get

$$
\begin{aligned}
& \mathbb{E}[B(\boldsymbol{y}_1^r, \boldsymbol{x}_1^s, k)\, B(\boldsymbol{y}_2^r, \boldsymbol{x}_2^s, k)] \\
= \quad & \lambda^2 \int_{K\in\mathbb{R}_+} \rho(K, 0) \Big(C(\boldsymbol{y}_1^r, \boldsymbol{y}_2^r, \mathcal{K}(K, k), k) C(\boldsymbol{x}_1^s, \boldsymbol{x}_2^s, \mathcal{K}(K, k), k) \\
& + C(\boldsymbol{y}_1^r, \boldsymbol{x}_2^s, \mathcal{K}(K, k), k) C(\boldsymbol{x}_1^s, \boldsymbol{y}_2^r, \mathcal{K}(K, k), k) \Big) dK \\
& + \lambda^2 \iint_{K_1, K_2\in\mathbb{R}_+} \rho\left(K_1, 0\right) \rho\left(K_2, 0\right) \\
& C(\boldsymbol{y}_1^r, \boldsymbol{x}_1^s, \mathcal{K}(K_1, k), k)\, C(\boldsymbol{y}_2^r, \boldsymbol{x}_2^s, \mathcal{K}(K_2, k), k) \\
& \times R_2\left((K_1 - K_2) \rho\left(\tfrac{K_1 + K_2}{2}, 0 \right) \right) dK_1 dK_2,
\end{aligned}
\tag{A.4}
$$

where we have used Eqs. (17) and (18). Finally, substituting Eqs. (43) and (A.4) into Eq. (A.3) yields

$$
\begin{aligned}
& \mathrm{cov}[B(\boldsymbol{y}_1^r, \boldsymbol{x}_1^s, k),\ \overline{B(\boldsymbol{y}_2^r, \boldsymbol{x}_2^s, k)}] \\
= \quad & \lambda^2 \int_{K\in\mathbb{R}_+} \rho(K, 0) \\
& \Big(C(\boldsymbol{y}_1^r, \boldsymbol{y}_2^r, \mathcal{K}(K, k), k) C(\boldsymbol{x}_1^s, \boldsymbol{x}_2^s, \mathcal{K}(K, k), k) \\
& + C(\boldsymbol{y}_1^r, \boldsymbol{x}_2^s, \mathcal{K}(K, k), k) C(\boldsymbol{x}_1^s, \boldsymbol{y}_2^r, \mathcal{K}(K, k), k) \Big) dK \\
& + \lambda^2 \iint_{K_1, K_2\in\mathbb{R}_+} \rho\left(K_1, 0\right) \rho\left(K_2, 0\right) \\
& C(\boldsymbol{y}_1^r, \boldsymbol{x}_1^s, \mathcal{K}(K_1, k), k)\, C(\boldsymbol{y}_2^r, \boldsymbol{x}_2^s, \mathcal{K}(K_2, k), k) \\
& \times \left(R_2\left((K_1 - K_2) \rho\left(\tfrac{K_1 + K_2}{2}, 0 \right) \right) - 1 \right) dK_1 dK_2.
\end{aligned}
$$

With the same change of variable $K_1 = K + \frac{s}{2\rho(K,0)}$ and $K_2 = K - \frac{s}{2\rho(K,0)}$ as in Sec. 3.1.3, we get asymptotically

$$
\begin{aligned}
& \mathrm{cov}[B(\boldsymbol{y}_1^r, \boldsymbol{x}_1^s, k),\ \overline{B(\boldsymbol{y}_2^r, \boldsymbol{x}_2^s, k)}] \\
= \quad & \lambda^2 \int_{K\in\mathbb{R}_+} \rho(K, 0) \Big(\\
& \Big(C(\boldsymbol{y}_1^r, \boldsymbol{y}_2^r, \mathcal{K}(K, k), k) C(\boldsymbol{x}_1^s, \boldsymbol{x}_2^s, \mathcal{K}(K, k), k)
\end{aligned}
$$

$$
\begin{aligned}
&+C(\boldsymbol{y}_1^r, \boldsymbol{x}_2^s, \mathcal{K}(K,k), k) C(\boldsymbol{x}_1^s, \boldsymbol{y}_2^r, \mathcal{K}(K,k), k)\Big) \\
&- \textstyle\int_{s\in\mathbb{R}} C(\boldsymbol{y}_1^r, \boldsymbol{x}_1^s, \mathcal{K}(K + \frac{s}{2\rho(K,0)}, k), k) \\
&\times C(\boldsymbol{y}_2^r, \boldsymbol{x}_2^s, \mathcal{K}(K - \frac{s}{2\rho(K,0)}, k), k) \times Y(s)\, ds\Big) dK,
\end{aligned}
$$

where we have substituted Eq. (20). In Sec. 4.3.2, we showed that the asymptotic statistics of the RIR when $t \to +\infty$ correspond to $b = \widehat{Y} = 0$, so the previous equation can be simplified by taking $Y = 0$:

$$
\begin{aligned}
& \operatorname{cov}[B(\boldsymbol{y}_1^r, \boldsymbol{x}_1^s, k),\ \overline{B(\boldsymbol{y}_2^r, \boldsymbol{x}_2^s, k)}] \\
= \;& \lambda^2 \textstyle\int_{K\in\mathbb{R}_+} \rho(K,0) \\
& \Big(C(\boldsymbol{y}_1^r, \boldsymbol{y}_2^r, \mathcal{K}(K,k), k)\, C(\boldsymbol{x}_1^s, \boldsymbol{x}_2^s, \mathcal{K}(K,k), k) \\
& + C(\boldsymbol{y}_1^r, \boldsymbol{x}_2^s, \mathcal{K}(K,k), k)\, C(\boldsymbol{x}_1^s, \boldsymbol{y}_2^r, \mathcal{K}(K,k), k)\Big) dK.
\end{aligned}
$$

Finally, substituting Eq. (14) and applying the change of variable $\kappa = \mathcal{K}(K,k)$ yields

$$
\begin{aligned}
& \operatorname{cov}[B(\boldsymbol{y}_1^r, \boldsymbol{x}_1^s, k), \overline{B(\boldsymbol{y}_2^r, \boldsymbol{x}_2^s, k)}] \\
= \;& \lambda^2 \textstyle\int_{K\in\mathbb{R}_+} \rho(\mathcal{K}(K,k), k) \dot{\mathcal{K}}(K,k) \\
& \Big(C(\boldsymbol{y}_1^r, \boldsymbol{y}_2^r, \mathcal{K}(K,k), k)\, C(\boldsymbol{x}_1^s, \boldsymbol{x}_2^s, \mathcal{K}(K,k), k) \\
& + C(\boldsymbol{y}_1^r, \boldsymbol{x}_2^s, \mathcal{K}(K,k), k)\, C(\boldsymbol{x}_1^s, \boldsymbol{y}_2^r, \mathcal{K}(K,k), k)\Big) dK \\
= \;& \lambda^2 \textstyle\int_{\kappa\in\mathcal{K}(\mathbb{R}_+,k)} \Big(C(\boldsymbol{y}_1^r, \boldsymbol{y}_2^r, \kappa, k)\, C(\boldsymbol{x}_1^s, \boldsymbol{x}_2^s, \kappa, k) \\
& + C(\boldsymbol{y}_1^r, \boldsymbol{x}_2^s, \kappa, k)\, C(\boldsymbol{x}_1^s, \boldsymbol{y}_2^r, \kappa, k)\Big) \rho(\kappa, k) d\kappa \\
= \;& \lambda^2 \textstyle\int_{\kappa\in\mathbb{R}_+} \Big(C(\boldsymbol{y}_1^r, \boldsymbol{y}_2^r, \kappa, k)\, C(\boldsymbol{x}_1^s, \boldsymbol{x}_2^s, \kappa, k) \\
& + C(\boldsymbol{y}_1^r, \boldsymbol{x}_2^s, \kappa, k)\, C(\boldsymbol{x}_1^s, \boldsymbol{y}_2^r, \kappa, k)\Big) \rho(\kappa, k) d\kappa,
\end{aligned}
$$

where the last equality is obtained by applying Cauchy's integral theorem.

Let us now focus on the universal pseudo-correlation function defined in Eq. (26). When $\boldsymbol{x}_1^s = \boldsymbol{x}_2^s = \boldsymbol{x}^s$, we then get the simplification:

$$
\begin{aligned}
& \operatorname{cov}[B(\boldsymbol{y}_1^r, \boldsymbol{x}^s, k), \overline{B(\boldsymbol{y}_2^r, \boldsymbol{x}^s, k)}] \\
= \;& \lambda^2 \textstyle\int_{\kappa\in\mathbb{R}_+} \Big(C(\boldsymbol{y}_1^r, \boldsymbol{y}_2^r, \kappa, k) + C(\boldsymbol{y}_1^r, \boldsymbol{x}^s, \kappa, k)\, C(\boldsymbol{x}^s, \boldsymbol{y}_2^r, \kappa, k)\Big) \rho(\kappa, k) d\kappa.
\end{aligned}
$$

Finally, if $\boldsymbol{y}_1^r$ and $\boldsymbol{y}_2^r$ are not too close to $\boldsymbol{x}^s$, then the terms $C(\boldsymbol{y}_1^r, \boldsymbol{x}^s, \kappa, k)$ and $C(\boldsymbol{x}^s, \boldsymbol{y}_2^r, \kappa, k)$ are of order $O(\frac{1}{\kappa})$, therefore their product, which is of order $O(\frac{1}{\kappa^2})$, can be neglected w.r.t. $C(\boldsymbol{y}_1^r, \boldsymbol{y}_2^r, \kappa, k)$, which is of order $O(\frac{1}{\kappa})$. By substituting Eq. (26), we thus get

$$
\operatorname{cov}[B(\boldsymbol{y}_1^r, \boldsymbol{x}^s, k), \overline{B(\boldsymbol{y}_2^r, \boldsymbol{x}^s, k)}] = \lambda^2 \textstyle\int_{\kappa\in\mathbb{R}_+} \operatorname{sinc}(2\pi\kappa \|\boldsymbol{y}_1^r - \boldsymbol{y}_2^r\|_2) \rho(\kappa, k) d\kappa. \tag{A.5}
$$

Note that this PCF is a function of $\boldsymbol{z} \triangleq \boldsymbol{y}_1^r - \boldsymbol{y}_2^r$, and that it is independent of the source position $\boldsymbol{x}^s$. We have thus finally proved the property that was originally introduced as the third assumption of the statistical wave field theory in Badeau (2024): the B-function behaves asymptotically like a centered pseudo-stationary random process, whose PCF is expressed as

$$J_B(\boldsymbol{z}, k) = \int_{\kappa\in\mathbb{R}_+} \mathrm{sinc}(2\pi\kappa\|\boldsymbol{z}\|_2)\widehat{J}_B(\kappa, k)d\kappa, \tag{A.6}$$

where $\widehat{J}_B(\kappa, k)$ is the *pseudo-spectrum* [Eq. (A.6) follows from Badeau (2024, Eq. (104), applied to $\widehat{\psi}(\boldsymbol{z}) = \delta(\boldsymbol{z}-\boldsymbol{z}_0)$)]. Finally, comparing Eqs. (A.5) and (A.6) shows that $\widehat{J}_B(\kappa, k) = \lambda^2\,\rho(\kappa, k)$, which is exactly the same as in Badeau (2024, Eq. (98)).

Appendix B. Statistics of the RIR

In this appendix, we calculate the first order statistics (Appendix B.1) and second order statistics (Appendix B.2) of the RIR presented in Sec. 4.3.

Appendix B.1. Mathematical expectation

If we consider the universal pseudo-correlation function in Eq. (26) along with the modal density in Eq. (13), as explained in Sec. 3.3, then substituting Eq. (51) into Eq.(54) yields

$$\begin{aligned}
\mathbb{E}[g(\boldsymbol{x}^r, \boldsymbol{x}^s, t)] = \;& \int_{f\in\mathbb{R}} \frac{\cos(2\pi\frac{f}{c}\|\boldsymbol{x}^r-\boldsymbol{x}^s\|_2)}{4\pi\|\boldsymbol{x}^r-\boldsymbol{x}^s\|_2} e^{\imath 2\pi f t} df \\
& +\epsilon\lambda S(\partial V)\int_{f\in\mathbb{R}} \frac{\mathrm{Si}(2\pi\frac{f}{c}\|\boldsymbol{x}^r-\boldsymbol{x}^s\|_2)}{4\pi\frac{f}{c}} \\
& \times\frac{\cos(2\pi\frac{f}{c}\|\boldsymbol{x}^r-\boldsymbol{x}^s\|_2)}{4\pi\|\boldsymbol{x}^r-\boldsymbol{x}^s\|_2} - \frac{\mathrm{Ci}(2\pi\frac{|f|}{c}\|\boldsymbol{x}^r-\boldsymbol{x}^s\|_2)}{4\pi\frac{f}{c}} \\
& \times\frac{\sin(2\pi\frac{f}{c}\|\boldsymbol{x}^r-\boldsymbol{x}^s\|_2)}{4\pi\|\boldsymbol{x}^r-\boldsymbol{x}^s\|_2} e^{\imath 2\pi f t} df \\
= \;& \frac{1}{4\pi\|\boldsymbol{x}^r-\boldsymbol{x}^s\|_2}\int_{f\in\mathbb{R}} \\
& \frac{e^{\imath 2\pi f (t-\frac{\|\boldsymbol{x}^r-\boldsymbol{x}^s\|_2}{c})}+e^{\imath 2\pi f (t+\frac{\|\boldsymbol{x}^r-\boldsymbol{x}^s\|_2}{c})}}{2} df \\
& +\frac{\epsilon\lambda S(\partial V)}{4\pi\|\boldsymbol{x}^r-\boldsymbol{x}^s\|_2}\int_{f\in\mathbb{R}} \Bigg(\frac{\mathrm{Si}(2\pi\frac{f}{c}\|\boldsymbol{x}^r-\boldsymbol{x}^s\|_2)}{4\pi\frac{f}{c}} \\
& \times\frac{e^{\imath 2\pi f (t-\frac{\|\boldsymbol{x}^r-\boldsymbol{x}^s\|_2}{c})}+e^{\imath 2\pi f (t+\frac{\|\boldsymbol{x}^r-\boldsymbol{x}^s\|_2}{c})}}{2} \\
& +\frac{\mathrm{Ci}(2\pi\frac{|f|}{c}\|\boldsymbol{x}^r-\boldsymbol{x}^s\|_2)}{4\pi\frac{f}{c}} \\
& \times\frac{e^{\imath 2\pi f (t-\frac{\|\boldsymbol{x}^r-\boldsymbol{x}^s\|_2}{c})}-e^{\imath 2\pi f (t+\frac{\|\boldsymbol{x}^r-\boldsymbol{x}^s\|_2}{c})}}{2\imath}\Bigg) df \\
= \;& \frac{\delta(t-\frac{\|\boldsymbol{x}^r-\boldsymbol{x}^s\|_2}{c})+\delta(t+\frac{\|\boldsymbol{x}^r-\boldsymbol{x}^s\|_2}{c})}{8\pi\|\boldsymbol{x}^r-\boldsymbol{x}^s\|_2} \\
& +\frac{\epsilon\lambda c S(\partial V)}{8\pi\|\boldsymbol{x}^r-\boldsymbol{x}^s\|_2}\int_{\tau=0}^{t}\int_{f\in\mathbb{R}} \Big(\imath\,\mathrm{Si}(2\pi\tfrac{f}{c}\|\boldsymbol{x}^r-\boldsymbol{x}^s\|_2) \\
& \times\frac{e^{\imath 2\pi f (\tau-\frac{\|\boldsymbol{x}^r-\boldsymbol{x}^s\|_2}{c})}+e^{\imath 2\pi f (\tau+\frac{\|\boldsymbol{x}^r-\boldsymbol{x}^s\|_2}{c})}}{2} \\
& +\mathrm{Ci}(2\pi\tfrac{|f|}{c}\|\boldsymbol{x}^r-\boldsymbol{x}^s\|_2) \\
& \times\frac{e^{\imath 2\pi f (\tau-\frac{\|\boldsymbol{x}^r-\boldsymbol{x}^s\|_2}{c})}-e^{\imath 2\pi f (\tau+\frac{\|\boldsymbol{x}^r-\boldsymbol{x}^s\|_2}{c})}}{2}\Big) df\,d\tau,
\end{aligned}$$

where we have expressed a function of time t as the primitive integral of its derivative in the last equality. Then, an integration by parts yields

$$
\begin{aligned}
&\mathbb{E}[g(\boldsymbol{x}^r,\boldsymbol{x}^s,t)] - \frac{\delta(t-\frac{\|\boldsymbol{x}^r-\boldsymbol{x}^s\|_2}{c})+\delta(t+\frac{\|\boldsymbol{x}^r-\boldsymbol{x}^s\|_2}{c})}{8\pi\|\boldsymbol{x}^r-\boldsymbol{x}^s\|_2}\\
= \;& -\frac{\epsilon\lambda c S(\partial V)}{8\pi\|\boldsymbol{x}^r-\boldsymbol{x}^s\|_2}\int_{\tau=0}^{t}\int_{f\in\mathbb{R}}\Bigg(\imath\frac{\sin(2\pi\frac{f}{c}\|\boldsymbol{x}^r-\boldsymbol{x}^s\|_2)}{f}\\
&\times\frac{\frac{e^{\imath 2\pi f(\tau-\frac{\|\boldsymbol{x}^r-\boldsymbol{x}^s\|_2}{c})}}{\imath 2\pi(\tau-\frac{\|\boldsymbol{x}^r-\boldsymbol{x}^s\|_2}{c})}+\frac{e^{\imath 2\pi f(\tau+\frac{\|\boldsymbol{x}^r-\boldsymbol{x}^s\|_2}{c})}}{\imath 2\pi(\tau+\frac{\|\boldsymbol{x}^r-\boldsymbol{x}^s\|_2}{c})}}{2}\\
&+\frac{\cos(2\pi\frac{f}{c}\|\boldsymbol{x}^r-\boldsymbol{x}^s\|_2)}{f}\\
&\times\frac{\frac{e^{\imath 2\pi f(\tau-\frac{\|\boldsymbol{x}^r-\boldsymbol{x}^s\|_2}{c})}}{\imath 2\pi(\tau-\frac{\|\boldsymbol{x}^r-\boldsymbol{x}^s\|_2}{c})}-\frac{e^{\imath 2\pi f(\tau+\frac{\|\boldsymbol{x}^r-\boldsymbol{x}^s\|_2}{c})}}{\imath 2\pi(\tau+\frac{\|\boldsymbol{x}^r-\boldsymbol{x}^s\|_2}{c})}}{2}\Bigg)df\,d\tau\\
= \;& -\frac{\epsilon\lambda c S(\partial V)}{16\pi\|\boldsymbol{x}^r-\boldsymbol{x}^s\|_2}\int_{\tau=0}^{t}\left(\frac{1}{\tau-\frac{\|\boldsymbol{x}^r-\boldsymbol{x}^s\|_2}{c}}-\frac{1}{\tau+\frac{\|\boldsymbol{x}^r-\boldsymbol{x}^s\|_2}{c}}\right)\\
&\times\left(\int_{f\in\mathbb{R}}\frac{e^{\imath 2\pi f\tau}}{\imath 2\pi f}df\right)d\tau\\
= \;& \frac{\epsilon\lambda c S(\partial V)}{32\pi\|\boldsymbol{x}^r-\boldsymbol{x}^s\|_2}\int_{\tau=0}^{t}\left(\frac{\mathrm{sign}(\tau)}{\tau+\frac{\|\boldsymbol{x}^r-\boldsymbol{x}^s\|_2}{c}}-\frac{\mathrm{sign}(\tau)}{\tau-\frac{\|\boldsymbol{x}^r-\boldsymbol{x}^s\|_2}{c}}\right)d\tau\\
= \;& \frac{\epsilon\lambda c S(\partial V)}{32\pi\|\boldsymbol{x}^r-\boldsymbol{x}^s\|_2}\,\mathrm{sign}(t)\,\ln\left|\frac{t+\frac{\|\boldsymbol{x}^r-\boldsymbol{x}^s\|_2}{c}}{t-\frac{\|\boldsymbol{x}^r-\boldsymbol{x}^s\|_2}{c}}\right|.
\end{aligned}
$$

We note that $\mathbb{E}[g(\boldsymbol{x}^r,\boldsymbol{x}^s,t)]$ is an even function of time, so $\mathbb{E}[h(\boldsymbol{x}^r,\boldsymbol{x}^s,t)]$ is obtained by adding to $\mathbb{E}[g(\boldsymbol{x}^r,\boldsymbol{x}^s,t)]$ the appropriate odd solution of the homogeneous wave equation [Eq. (1)], which is such that the resulting function is causal:

$$
\mathbb{E}[h(\boldsymbol{x}^r,\boldsymbol{x}^s,t)] = \mathbb{E}[g(\boldsymbol{x}^r,\boldsymbol{x}^s,t)] + \frac{\delta(t-\frac{\|\boldsymbol{x}^r-\boldsymbol{x}^s\|_2}{c})-\delta(t+\frac{\|\boldsymbol{x}^r-\boldsymbol{x}^s\|_2}{c})}{8\pi\|\boldsymbol{x}^r-\boldsymbol{x}^s\|_2} + \frac{\epsilon\lambda c S(\partial V)}{32\pi\|\boldsymbol{x}^r-\boldsymbol{x}^s\|_2}\ln\left|\frac{t+\frac{\|\boldsymbol{x}^r-\boldsymbol{x}^s\|_2}{c}}{t-\frac{\|\boldsymbol{x}^r-\boldsymbol{x}^s\|_2}{c}}\right|,
$$

which finally implies Eq. (58).

Appendix B.2. Second order moments

First, Eq. (6) yields

$$
\mathbb{E}[g(\boldsymbol{x}_1^r,\boldsymbol{x}_1^s,t_1)\,g(\boldsymbol{x}_2^r,\boldsymbol{x}_2^s,t_2)] = \iint_{f_1,f_2\in\mathbb{R}}\mathbb{E}[G(\boldsymbol{x}_1^r,\boldsymbol{x}_1^s,\tfrac{f_1}{c})\,\overline{G(\boldsymbol{x}_2^r,\boldsymbol{x}_2^s,\tfrac{f_2}{c})}]e^{\imath 2\pi f_1 t_1}\overline{e^{\imath 2\pi f_2 t_2}}df_1 df_2. \tag{B.1}
$$

Then, by substituting Eq. (53) into Eq. (B.1), we get

$$
\begin{aligned}
&\mathbb{E}[g(\boldsymbol{x}_1^r,\boldsymbol{x}_1^s,t_1)\,g(\boldsymbol{x}_2^r,\boldsymbol{x}_2^s,t_2)]\\
= \;& \frac{\lambda^2 c^4}{16\pi^4}\int_{K\in\mathbb{R}_+}\Bigg(\iint_{f_1,f_2\in\mathbb{R}}\frac{\gamma\left(\boldsymbol{x}_1^r,\boldsymbol{x}_2^r,K,\frac{f_1}{c},\frac{f_2}{c}\right)\overline{\gamma\left(\boldsymbol{x}_1^s,\boldsymbol{x}_2^s,K,\frac{f_1}{c},\frac{f_2}{c}\right)}}{\left(f_1^2-c^2\mathcal{K}\left(K,\frac{f_1}{c}\right)^2\right)\overline{\left(f_2^2-c^2\mathcal{K}\left(K,\frac{f_2}{c}\right)^2\right)}}\\
&+\frac{\gamma\left(\boldsymbol{x}_1^r,\boldsymbol{x}_2^s,K,\frac{f_1}{c},\frac{f_2}{c}\right)\overline{\gamma\left(\boldsymbol{x}_1^s,\boldsymbol{x}_2^r,K,\frac{f_1}{c},\frac{f_2}{c}\right)}}{\left(f_1^2-c^2\mathcal{K}\left(K,\frac{f_1}{c}\right)^2\right)\overline{\left(f_2^2-c^2\mathcal{K}\left(K,\frac{f_2}{c}\right)^2\right)}}\\
&\times e^{\imath 2\pi f_1 t_1}\overline{e^{\imath 2\pi f_2 t_2}}\,df_1 df_2
\end{aligned}
$$

$$
\begin{aligned}
&+\int_{s\in\mathbb{R}}\int_{f_1\in\mathbb{R}}\int_{f_2\in\mathbb{R}} \frac{C(\boldsymbol{x}_1^r,\boldsymbol{x}_1^s,\mathcal{K}(K+\frac{s}{2\rho(K,0)},\frac{f_1}{c}),\frac{f_1}{c})}{\left(f_1^2-c^2\mathcal{K}\left(K+\frac{s}{2\rho(K,0)},\frac{f_1}{c}\right)^2\right)}\\
&\times\overline{\frac{C(\boldsymbol{x}_2^r,\boldsymbol{x}_2^s,\mathcal{K}(K-\frac{s}{2\rho(K,0)},\frac{f_2}{c}),\frac{f_2}{c})}{\left(f_2^2-c^2\mathcal{K}\left(K-\frac{s}{2\rho(K,0)},\frac{f_2}{c}\right)^2\right)}}\\
&\times e^{\imath 2\pi f_1 t_1}\overline{e^{\imath 2\pi f_2 t_2}}df_1 df_2\,(1-Y(s))\,ds\Big)\rho(K,0)dK,
\end{aligned}
$$

where the level cluster function $Y(s)$ was defined in Eq. (20).

Now, let us assume that $\mathrm{Re}(\widehat{\beta}) > 0$, and consider the function $\kappa(K)$ introduced in Eq. (59). Then Eq. (15) yields $\mathcal{K}(K, -\overline{\kappa(K)}) = \overline{\kappa(K)}$. Therefore the equation $f^2 = c^2\mathcal{K}(K, \frac{f}{c})^2$ admits two solutions, $f = c\kappa(K)$ and $f = -c\overline{\kappa(K)}$, which are both in the upper half complex plane. Then by applying the residue theorem to calculate the integrals w.r.t. f_1 and f_2, we get[4]

$$
\begin{aligned}
&\mathbb{E}[g(\boldsymbol{x}_1^r,\boldsymbol{x}_1^s,t_1)\,g(\boldsymbol{x}_2^r,\boldsymbol{x}_2^s,t_2)]\\
=\;&\frac{\lambda^2c^2}{8\pi^2}H(t_1)H(t_2)\,\mathrm{Re}\int_{K\in\mathbb{R}_+}\\
&\Big(\frac{\gamma(\boldsymbol{x}_1^r,\boldsymbol{x}_2^r,\kappa(K))\,\gamma(\boldsymbol{x}_1^s,\boldsymbol{x}_2^s,\kappa(K))}{|\kappa(K)|^2}\\
&+\frac{\gamma(\boldsymbol{x}_1^r,\boldsymbol{x}_2^s,\kappa(K))\,\gamma(\boldsymbol{x}_1^s,\boldsymbol{x}_2^r,\kappa(K))}{|\kappa(K)|^2}e^{\imath 2\pi c\left(\kappa(K)t_1-\overline{\kappa(K)}t_2\right)}\\
&+\int_{s\in\mathbb{R}}\frac{C(\boldsymbol{x}_1^r,\boldsymbol{x}_1^s,\kappa(K+\frac{s}{2\rho(K,0)}))}{\kappa\left(K+\frac{s}{2\rho(K,0)}\right)}\,\overline{\frac{C(\boldsymbol{x}_2^r,\boldsymbol{x}_2^s,\kappa(K-\frac{s}{2\rho(K,0)}))}{\kappa\left(K-\frac{s}{2\rho(K,0)}\right)}}\\
&\times e^{\imath 2\pi c\left(\kappa\left(K+\frac{s}{2\rho(K,0)}\right)t_1-\overline{\kappa\left(K-\frac{s}{2\rho(K,0)}\right)}t_2\right)}\\
&\times(1-Y(s))\,ds\Big)\rho(K,0)dK,
\end{aligned}
\tag{B.2}
$$

where notations $C(\boldsymbol{x}_1, \boldsymbol{x}_2, \kappa)$ and $\gamma(\boldsymbol{x}_1, \boldsymbol{x}_2, \kappa)$ were introduced in Eqs. (66) and (67), respectively, and, due to the high frequency assumption, we have neglected the terms that depend on t_1 and t_2 only through $e^{\imath 2\pi c\kappa(.)\,(t_1+t_2)}$, which correspond to the zero frequency in the cross-Wigner time-frequency distribution introduced in Sec. 3.4.

In other respects, we note the presence of the Heaviside function $H(.)$ in Eq. (B.2), which shows that the function $g(\boldsymbol{x}^r, \boldsymbol{x}^s, t)$ that appears in this equation is actually the causal solution to the inhomogeneous wave equation [Eq. (3)], so it is by definition equal to the RIR $h(\boldsymbol{x}^r, \boldsymbol{x}^s, t)$. So, in the rest of this section, $g(\boldsymbol{x}^r, \boldsymbol{x}^s, t)$ will be replaced by $h(\boldsymbol{x}^r, \boldsymbol{x}^s, t)$.

When $K \to +\infty$, the terms $\kappa\left(K \pm \frac{s}{2\rho(K,0)}\right)$ in Eq. (B.2) will be approximated either by the first order Taylor expansion $\kappa(K) \pm \frac{s}{2\rho(K,0)}$, given that $\rho(K, 0) \to +\infty$ and that the derivative $\dot{\kappa}(K) \to 1$ asymptotically, when they are multiplied by a time, or more simply by the zeroth order Taylor expansion $\kappa(K)$ when they are not. Equation (B.2) then yields

[4] In each integral, the two poles lie in the interior of the upper half complex plane, the integration contour contains an interval of $\mathbb{R}$ centered at $f = 0$, and this contour is included in the upper half complex plane.

$$
\begin{aligned}
& \mathbb{E}[h(\boldsymbol{x}_1^r, \boldsymbol{x}_1^s, t_1)\, h(\boldsymbol{x}_2^r, \boldsymbol{x}_2^s, t_2)] \\
= \; & \tfrac{\lambda^2 c^2}{8\pi^2} H(t_1) H(t_2) \,\mathrm{Re} \int_{K \in \mathbb{R}_+} \\
& \Big(\gamma(\boldsymbol{x}_1^r, \boldsymbol{x}_2^r, \kappa(K))\, \gamma(\boldsymbol{x}_1^s, \boldsymbol{x}_2^s, \kappa(K)) \\
& + \gamma(\boldsymbol{x}_1^r, \boldsymbol{x}_2^s, \kappa(K))\, \overline{\gamma(\boldsymbol{x}_1^s, \boldsymbol{x}_2^r, \kappa(K))} \\
& + C(\boldsymbol{x}_1^r, \boldsymbol{x}_1^s, \kappa(K))\, \overline{C(\boldsymbol{x}_2^r, \boldsymbol{x}_2^s, \kappa(K))} \\
& \times \int_{s \in \mathbb{R}} e^{\imath 2\pi s \frac{c(t_1+t_2)}{2\rho(K,0)}} (1 - Y(s))\, ds \Big) \\
& \times \tfrac{e^{\imath 2\pi c \left(\kappa(K) t_1 - \overline{\kappa(K)} t_2\right)}}{|\kappa(K)|^2} \rho(K,0) dK.
\end{aligned}
$$

Then by noticing that function $b = \widehat{Y}$ defined in Eq. (21) is also the inverse Fourier transform of Y since it is real and even, we get

$$
\begin{aligned}
& \mathbb{E}[h(\boldsymbol{x}_1^r, \boldsymbol{x}_1^s, t_1)\, h(\boldsymbol{x}_2^r, \boldsymbol{x}_2^s, t_2)] \\
= \; & \tfrac{c^2}{8\pi^2} H(t_1) H(t_2) \,\mathrm{Re} \int_{K \in \mathbb{R}_+} \\
& \Big(\gamma(\boldsymbol{x}_1^r, \boldsymbol{x}_2^r, \kappa(K))\, \gamma(\boldsymbol{x}_1^s, \boldsymbol{x}_2^s, \kappa(K)) \\
& + \gamma(\boldsymbol{x}_1^r, \boldsymbol{x}_2^s, \kappa(K))\, \overline{\gamma(\boldsymbol{x}_1^s, \boldsymbol{x}_2^r, \kappa(K))} \\
& + C(\boldsymbol{x}_1^r, \boldsymbol{x}_1^s, \kappa(K))\, \overline{C(\boldsymbol{x}_2^r, \boldsymbol{x}_2^s, \kappa(K))} \\
& \times \left(\delta\left(\tfrac{t_1+t_2}{2t_H(K,0)}\right) - b\left(\tfrac{t_1+t_2}{2t_H(K,0)}\right)\right)\Big) \\
& \times \tfrac{e^{\imath 2\pi c \left(\kappa(K) t_1 - \overline{\kappa(K)} t_2\right)}}{|\kappa(K)|^2} \widehat{\Gamma}_B(K) dK,
\end{aligned}
\tag{B.3}
$$

where $t_H(K,0) = \frac{\rho(K,0)}{c}$ is the Heisenberg time that was defined in Eq. (31), and $\widehat{\Gamma}_B(K)$ is the power spectral density that was defined in Eq. (64).

Note that when $t_1, t_2 > 0$, then $t \triangleq \frac{t_1+t_2}{2} > 0$, so $\delta\left(\frac{t}{t_H(K,0)}\right) = 0$. Then, by applying the change of variable $K = (\mathrm{Re}\kappa)^{-1}(k)$, Eq. (B.3) finally yields Eq. (60).

References

Ahlfors, L. (**1979**). *Complex Analysis* (McGraw-Hill, New York, NY).

Badeau, R. (**2024**). “Statistical wave field theory,” J. Acoust. Soc. Am. **156**(1), 573–599.

Badeau, R. (**2025**a). “On the spectral decomposition of the complex Robin Laplacian,” J. Acoust. Soc. Am. **158**(1), 838–848.

Badeau, R. (**2025**b). “Statistical wave field theory: Curvature term,” J. Acoust. Soc. Am. **157**(3), 1650–1664.

Badeau, R. (**2026**a). “Statistical wave field theory: Anisotropic wave fields under Neumann’s boundary condition,” J. Acoust. Soc. Am. **159**(3), 2265–2280.

Badeau, R. (**2026**b). “Statistical wave field theory: Anisotropic wave fields under Robin’s boundary condition,” J. Acoust. Soc. Am. **159**(6), 5359–5377.

Badeau, R. (**2026**c). "Statistical wave field theory: main results," in *Proc. of Forum Acusticum 2026*, Graz, Austria.

Badeau, R. (**2026**d). "Statistical wave field theory: Random wave model of the complex Robin Laplacian," J. Acoust. Soc. Am. Under review.

Balian, R., and Bloch, C. (**1970**). "Distribution of eigenfrequencies for the wave equation in a finite domain: I. Three-dimensional problem with smooth boundary surface," Ann. Phys. **60**(2), 401–447.

Balian, R., and Bloch, C. (**1972**). "Distribution of eigenfrequencies for the wave equation in a finite domain: III. Eigenfrequency density oscillations," Ann. Phys. **69**(1), 76–160.

Berry, M. V. (**1977**). "Regular and irregular semiclassical wavefunctions," Journal of Physics A: Mathematical and General **10**(12), 2083–2091.

Cohen, L. (**1989**). "Time-frequency distributions-a review," Proc. IEEE **77**(7), 941–981.

Gutzwiller, M. C. (**1971**). "Periodic orbits and classical quantization conditions," Journal of Mathematical Physics **12**(3), 343–358.

Hortikar, S., and Srednicki, M. (**1998**). "Correlations in chaotic eigenfunctions at large separation," Phys. Rev. Lett. **80**(8), 1646–1649.

Janssen, P., and Stoica, P. (**1988**). "On the expectation of the product of four matrix-valued Gaussian random variables," IEEE Trans. Autom. Control **33**(9), 867–870.

Kuttruff, H. (**2014**). *Room Acoustics, 5th ed.* (CRC Press, Boca Raton, FL), pp. 1–374.

Lu, Z., Graf, A. M., Heller, E. J., Keski-Rahkonen, J., and Dag, C. B. (**2025**). "Antiscarring from eigenstate stacking in a chaotic spinor condensate," Phys. Rev. A **112**, 043307.

Mehta, M. (**1991**). *Random Matrices* (Academic Press, New York).

Morse, P. M., and Ingard, K. U. (**1968**). *Theoretical acoustics* (McGraw-Hill, New York, NY).

Prinn, A. G., and Badeau, R. (**2026**). "Verification of reverberation time predictions derived from the statistical wave field theory," Applied Acoustics **250**, 111337.

Tanner, G., and Søndergaard, N. (**2007**). "Wave chaos in acoustics and elasticity," J. Phys. A: Math. Theor. **40**, R443–R509.

Urbina, J. D., and Richter, K. (**2006**). "Statistical description of eigenfunctions in chaotic and weakly disordered systems beyond universality," Phys. Rev. Lett. **97**, 214101.

Urbina, J. D., and Richter, K. (**2007**). "Random wave functions with boundary and normalization constraints," Eur. Phys. J. Spec. Top. **145**, 255–269.

Weaver, R. L., and Lobkis, O. I. (**2000**). "Enhanced backscattering and modal echo of reverberant elastic waves," Phys. Rev. Lett. **84**(21), 4942–4945.

Weyl, H. (**1911**). "Ueber die asymptotische verteilung der eigenwerte (*On the asymptotic distribution of eigenvalues*)," Nachr. von der Gesellschaft der Wissenschaften zu Göttingen, Mathematisch-Physikalische Klasse **1911**, 110–117.

Zelditch, S. (**2006**). "Quantum ergodicity and mixing of eigenfunctions," in *Encyclopedia of mathematical physics*, edited by J.-P. Françoise, G. L. Naber, and T. S. Tsun, **1** (Academic Press/Elsevier Science, Oxford, UK).

Zelditch, S., and Zworski, M. (**1996**). "Ergodicity of eigenfunctions for ergodic billiards," Communications in Mathematical Physics **175**(3), 673–682.